nature communications

Article

https://doi.org/10.1038/s41467-024-52818-0

Coronavirus envelope protein activates TMED10-mediated unconventional secretion of inflammatory factors

Received: 30 March 2024

Accepted: 20 September 2024

Published online: 08 October 2024

Check for updates

Lei Liu[1,2,5], Lijingyao Zhang[1,3,5], Xinyan Hao[1,2], Yang Wang[1,3], Xiaochun Zhang[2], Liang Ge[1,3], Peihui Wang[4], Boxue Tian[2] & Min Zhang[1,2]

The precise cellular mechanisms underlying heightened proinflammatory cytokine production during coronavirus infection remain incompletely understood. Here we identify the envelope (E) protein in severe coronaviruses (SARS-CoV-2, SARS, or MERS) as a potent inducer of interleukin-1 release, intensifying lung inflammation through the activation of TMED10-mediated unconventional protein secretion (UcPS). In contrast, the E protein of mild coronaviruses (229E, HKU1, or OC43) demonstrates a less pronounced effect. The E protein of severe coronaviruses contains an SS/DS motif, which is not present in milder strains and facilitates interaction with TMED10. This interaction enhances TMED10-oligomerization, facilitating UcPS cargo translocation into the ER-Golgi intermediate compartment (ERGIC)—a pivotal step in interleukin-1 UcPS. Progesterone analogues were identified as compounds inhibiting E-enhanced release of proinflammatory factors and lung inflammation in a Mouse Hepatitis Virus (MHV) infection model. These findings elucidate a molecular mechanism driving coronavirus-induced hyperinflammation, proposing the E-TMED10 interaction as a potential therapeutic target to counteract the adverse effects of coronavirus-induced inflammation.

Excessive and uncontrolled proinflammatory cytokine production, notably evident in pathogen infections such as coronavirus (e.g., SARS-CoV-2, SARS, or MERS), can precipitate immunopathogenesis, resulting in widespread tissue damage, including acute lung injuries, across the human body[1–6]. This process correlates with the emergence of multiple organ dysfunction syndrome and an elevated likelihood of mortality[1–5]. The observed surge in proinflammatory cytokines, including interleukin-1 (IL1), interleukin-6 (IL6), interleukin-12 (IL12), interferon-gamma (IFNγ), and tumor necrosis factor-alpha (TNFα) circulates in the bloodstream. While these cytokines initially function as protective signals to activate the immune system, their excessive release significantly exacerbates the severity of the condition[2,3,6–9].

Among these inflammatory mediators, members of the IL1 family, notably IL1β and IL33, serve as crucial upstream regulators in the inflammatory cascade[10–12]. Prior studies on protein-protein interactions have indicated the potential for viral proteins from coronaviruses (e.g., SARS-CoV-2) to provoke the release of IL1s, including IL1β and IL33[13–15], both recognized for their engagement in unconventional protein secretion[16–18]. Gasdermins have been identified as key regulators in the release of IL1β and IL33. For example, acute bacterial infection leads to Gasdermin D (GSDMD) -dependent release of IL1β in macrophages, typically accompanied by pyroptosis[19–21]. Allergens can trigger GSDMD-mediated release of IL33 in epithelial cells[22], and helminth infection results in GSDMC-dependent release of IL33 in the

[1]State Key Laboratory of Membrane Biology, Tsinghua University, Beijing 100084, China. [2]School of Pharmaceutical Sciences, Tsinghua University, Beijing 100084, China. [3]Tsinghua University-Peking University Joint Center for Life Sciences, School of Life Sciences, Tsinghua University, Beijing 100084, China. [4]Key Laboratory for Experimental Teratology of Ministry of Education and Advanced Medical Research Institute, Meili Lake Translational Research Park, Cheeloo College of Medicine, Shandong University, Jinan 250012, China. [5]These authors contributed equally: Lei Liu, Lijingyao Zhang.
e-mail: zhangmin143@mail.tsinghua.edu.cn

intestin[23]. Additionally, the release of IL1β and IL33 can be regulated by GSDMD-independent pathways, including TMED10-mediated unconventional secretion, secretory autophagy and PIP2-dependent translocation like FGF2[17,24–26].

Nevertheless, a comprehensive molecular elucidation regarding how coronaviruses induce the unconventional release of inflammatory factors remains elusive, particularly considering the variability in infection outcomes among distinct coronaviruses. Lethal strains such as SARS-CoV-2, SARS-CoV, or MERS-CoV prompt heightened proinflammatory cytokine production, whereas coronaviruses like 229E, HKU1, or OC43 result in mild symptoms with reduced inflammation[27–29]. The intricate cellular mechanisms governing coronavirus modulation of host inflammatory responses, particularly the release of proinflammatory factors, remain incompletely understood, including the interplay between viral factors and host secretion systems leading to excessive inflammatory factor release at cellular and subcellular levels, and the distinctions between severe and mild viruses in this regard.

An intriguing aspect of coronavirus biology involves the utilization of the ER-Golgi intermediate compartment (ERGIC) as a packaging site, where various viral factors accumulate[30–32]. Previously, we identified a protein translocation pathway operating within the ERGIC, responsible for the unconventional release of multiple inflammatory factors, including members of the IL1 family[17]. This pathway, termed TMED10-channeled unconventional protein secretion (THU), relies on the ERGIC-localized TMED10 protein to facilitate the entry of IL1 family factors into the secretory system, initiating unconventional secretion[17]. Our prior investigations underscored the regulatory role of THU in inflammatory responses to bacterial infections and colitis[17,33].

In this study, we discovered that the E proteins from severe coronaviruses (SARS-CoV-2, SARS, and MERS) markedly stimulate the release of inflammatory factors, exacerbating lung inflammation through THU, whereas mild strains exert less impact. Mechanistically, the interaction between E proteins and TMED10 promotes TMED10 oligomerization, facilitating the translocation of UcPS cargo into the ERGIC—an essential step in interleukin-1 UcPS. We identified a specific SS/DS motif on the E proteins of severe coronaviruses crucial for TMED10 interaction and the subsequent triggering of excessive inflammatory factor release. Significantly, through screening of FDA-approved drugs, we identified progesterone analogs that mainly function to disrupt the E-TMED10 interaction, effectively reducing proinflammatory factor release and lung inflammation in a MHV infection model. These findings highlight the E-TMED10 interaction as a promising therapeutic target, with progesterone analogs showing potential as lead compounds for developing anti-hyperinflammatory agents to mitigate the adverse effects of coronavirus-induced inflammation.

Results

Coronavirus E protein promotes UcPS

To elucidate the mechanisms by which coronavirus proteins induce UcPS of inflammatory factors, we conducted an examination focusing on the influence of individual SARS2 proteins on the secretion of mature IL1β (mIL1β). This assessment employed a previously established secretion system[34].Remarkably, the expression of the E protein was found to enhance IL1β secretion, while the other SARS-CoV-2 factors (N, S, M, ORF3a, ORF6, ORF7b, and ORF8) exhibited comparatively lesser effects (Fig. 1a, b). The effect of the E protein on IL1β secretion was found to be dose-dependent (Supplementary Fig. 1a), and this effect was independent of the specific tag used, as both untagged and Myc or Flag-tagged E consistently enhanced IL1β secretion (Supplementary Fig. 1b). Additionally, the E protein also promoted the UcPS of other IL1 family inflammatory factors, including IL33, IL36α, IL1α, and IL18, while it had no influence on the secretion of conventional cargo IL6 (Fig. 1c).

Previous studies showed SARS-CoV-2 infection can cause host inflammation through GSDMD-mediated pyroptosis by activating inflammasomes, which cleave GSDMD, triggering cell lysis and the release of pro-inflammatory cytokines including IL1β and IL18, thereby amplifying the inflammatory response[35–37]. Interestingly, when E protein expression was tested in GSDMD knockout THP-1 cells, it was found to enhance the secretion of mature IL1β, suggesting that E-regulated UcPS is independent of GSDMD (Fig. 1d). Furthermore, E protein expression had minimal effect on Caspase-3 cleavage or LDH release, indicating that the E-regulated UcPS is not attributed to cell death (Supplementary Fig. 1a).

To investigate whether E proteins from various coronaviruses impact UcPS, we assessed the secretion of mIL1β in both non-inflammatory and inflammatory cell contexts. Surprisingly, we observed that E proteins from severe symptom-causing coronaviruses (Es-SSC), including SARS-CoV-2, SARS, and MERS, strongly enhanced mIL1β secretion, while those from mild symptom-causing coronaviruses (Es-MSC), such as 229E, HKU1, and OC43, had a moderate effect (Fig. 1e, f). A similar trend was noted in the stimulation of mIL33 secretion, both in non-inflammatory cells and BEAS-2B lung bronchial epithelial cells (Fig. 1g, h).

To elucidate the role of the E protein in promoting inflammation within physiological settings, we expressed the E proteins of SARS-CoV-2 (E-SARS2, an example of Es-SSC) and 229E (E-229E, an example of Es-MSC) in the lungs of C57BL/6 mice using Adeno-Associated Virus (AAV)[38] (Fig. 1k, left panel). Following a moderate challenge with lipopolysaccharide (LPS), we found that E-SARS2, but not E-229E, expression led to an increase in inflammation, evidenced by elevated serum levels of IL1β (Fig. 1i). This was accompanied by a corresponding rise in IL6 production in the lung, kidney, liver, and spleen (Fig. 1j). Additionally, the expression of E-SARS2, as opposed to E-229E, enhanced the infiltration of immune cells into the lung (Fig. 1k, middle and right panel, and 1 l). These findings suggest that coronavirus E proteins promote the UcPS of inflammatory factors, and the impact of different E proteins correlates with the severity of symptoms following infection.

Previously documented evidence has established the coronavirus E protein's role as a viroporin[5,39–43], forming an ion channel capable of activating the inflammasome and potentially enhancing the maturation and secretion of IL1β[44,45]. Contrary to expectations, both E-SARS2 and E-SARS, even when engineered with mutations eliminating ion channel activity[5,41,46–48], exhibited the same efficiency in promoting the secretion of mIL1β-HA as the wild-type (WT) E protein in non-inflammatory cells (Fig. 1m–o). These findings suggest that ion channel activity is unlikely to directly regulate the secretion of mIL1β itself. Notably, the T9I mutation in the E protein, present in the omicron strain of SARS-CoV-2[42,49], did not impact the effect of E on UcPS (Fig. 1m). However, this mutation significantly decreased stability (Supplementary Fig. 1c, d), potentially compromising sustained UcPS triggered by E. The destabilization together with a compromised channel activity likely contributes to decreased inflammation upon omicron infection[42,50,51].

E-regulated UcPS is dependent on TMED10

Previous research has established that the coronavirus E protein primarily localizes to the ERGIC[31,32,43,52], a compartment we've identified as a pivotal station in the regulation of IL1 family members' secretion through an UcPS pathway termed TMED10-channeled UcPS (THU)[17]. Importantly, E proteins from both severe and mild symptom-causing coronaviruses are found to be concentrated on the ERGIC (Fig. 2a). Notably, E-SARS2 was observed to co-localize with TMED10 on the ERGIC (Fig. 2b), suggesting that E-mediated regulation of UcPS may be linked to the THU pathway. Intriguingly, E-SARS2 failed to enhance the secretion of mIL1β in TMED10 knockout (KO) cells (Fig. 2c), a pattern

https://doi.org/10.1038/s41467-024-52818-0

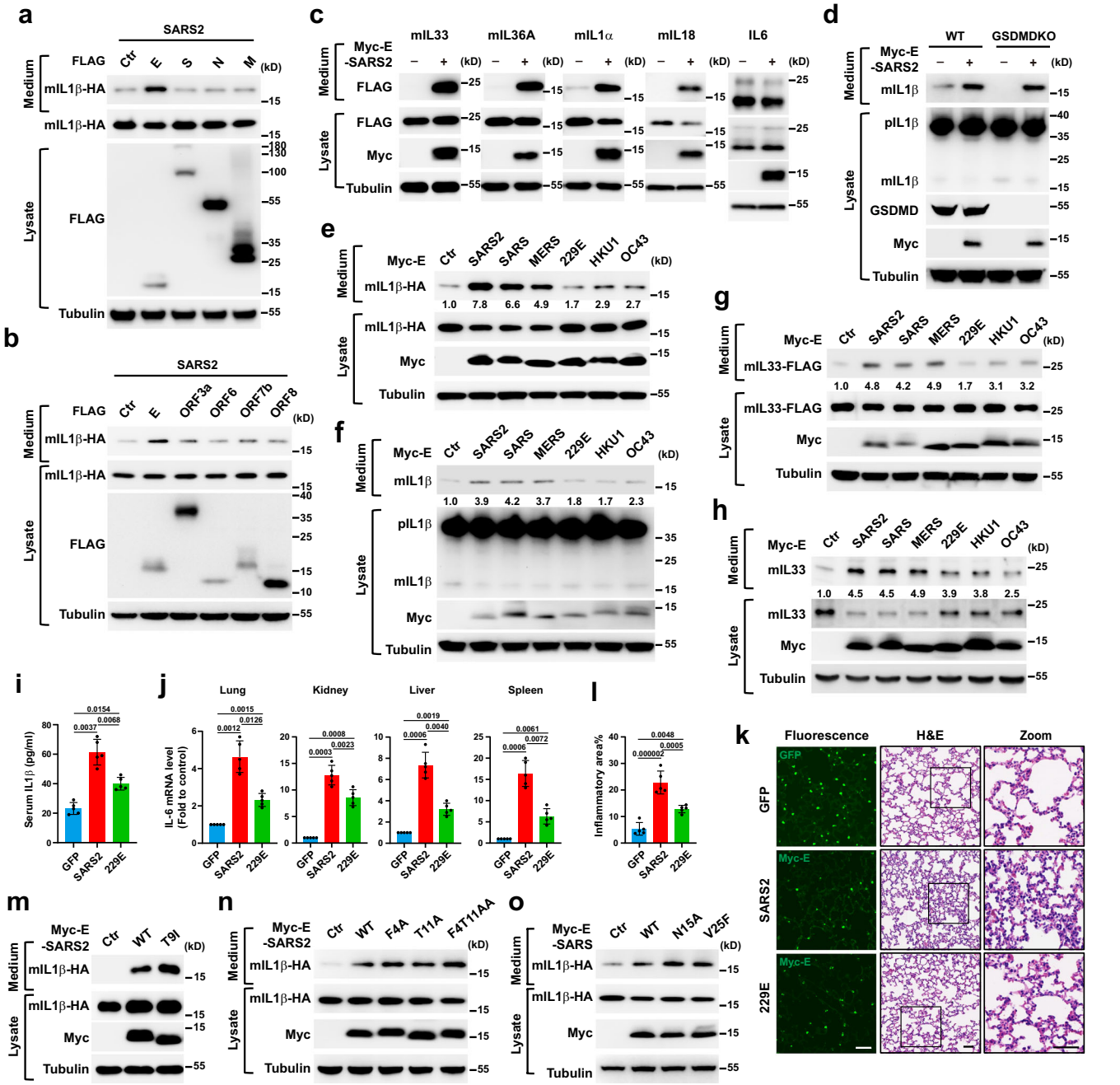

Fig. 1 | Coronavirus E protein promotes UcPS. a, **b** mIL1β-HA secretion in HEK293T cells transfected with mIL1β-HA alone or together with FLAG-tagged SARS2 proteins as indicated. **c** Secretion of mature IL1s and IL6 in HEK293T cells with or without Myc-tagged E-SARS2 expression. **d** mIL1β secretion in WT or GSDMD-KO THP-1 cells with or without Myc-tagged E-SARS2 expression. **e** Secretion of mIL1β-HA in HEK293T cells transfected with mIL1β-HA alone or together with Myc-tagged E of indicated coronaviruses. **f** mIL1β secretion in THP-1 cells expressed with or without Myc-tagged E of indicated coronaviruses. **g** Secretion of mIL33-FLAG in HEK293T cells transfected with mIL33-FLAG alone or together with Myc-tagged E of indicated coronaviruses. **h** mIL33 secretion in BEAS-2B cells expressed with or without Myc-tagged E of indicated coronaviruses. **i**–**l** C57BL/6 WT mice injected with AAV-GFP, AAV-Myc-E-SARS2 or AAV-Myc-E-229E were challenged with 15 mg/kg LPS for 15 h and euthanized. Expression of Myc-E-SARS2, Myc-E-229E or GFP in the lung was verified by immunofluorescence (**k**, left panel). Serum IL1β levels were determined by ELISA in (**i**). IL6 mRNA levels in indicated tissues were analyzed in (**j**). Lung inflammation was analyzed by H&E staining (**k**, middle and right panel) and inflammatory area was quantified in (**l**). **m**–**o** mIL1β-HA secretion in HEK293T cells transfected with mIL1β-HA alone or together with Myc-tagged E WT or indicated ion channel (IC) mutants of SARS2 (**m**, **n**) or SARS (**o**). The secretion levels of mIL1β or mIL33 were quantified based on the band intensities in the medium using Image J (**e**–**h**). Data are mean ± s.d. Statistical significance was assessed using one-way ANOVA ($n = 5$) followed by Tukey's multiple-comparison test. P values are indicated. Scale bars, 50 μm. Source data are provided as a Source Data file.

similarly observed in the secretion of mIL33 and mIL36α (Supplementary Fig. 2a, b).

Further analysis of endogenous mIL1β and mIL33 secretion in THP-1 or BEAS-2B cells revealed that E-regulated UcPS was substantially impaired in the absence of TMED10, an effect that could be restored upon TMED10 re-expression (Fig. 2d, e). This finding further confirms that E-SARS2 promotes UcPS through the THU pathway. In mice lacking TMED10, the expression of E-SARS2 failed to increase serum IL1β levels, as well as the production of IL6 and lung injury resulting from immune cell infiltration, in comparison to their WT

https://doi.org/10.1038/s41467-024-52818-0

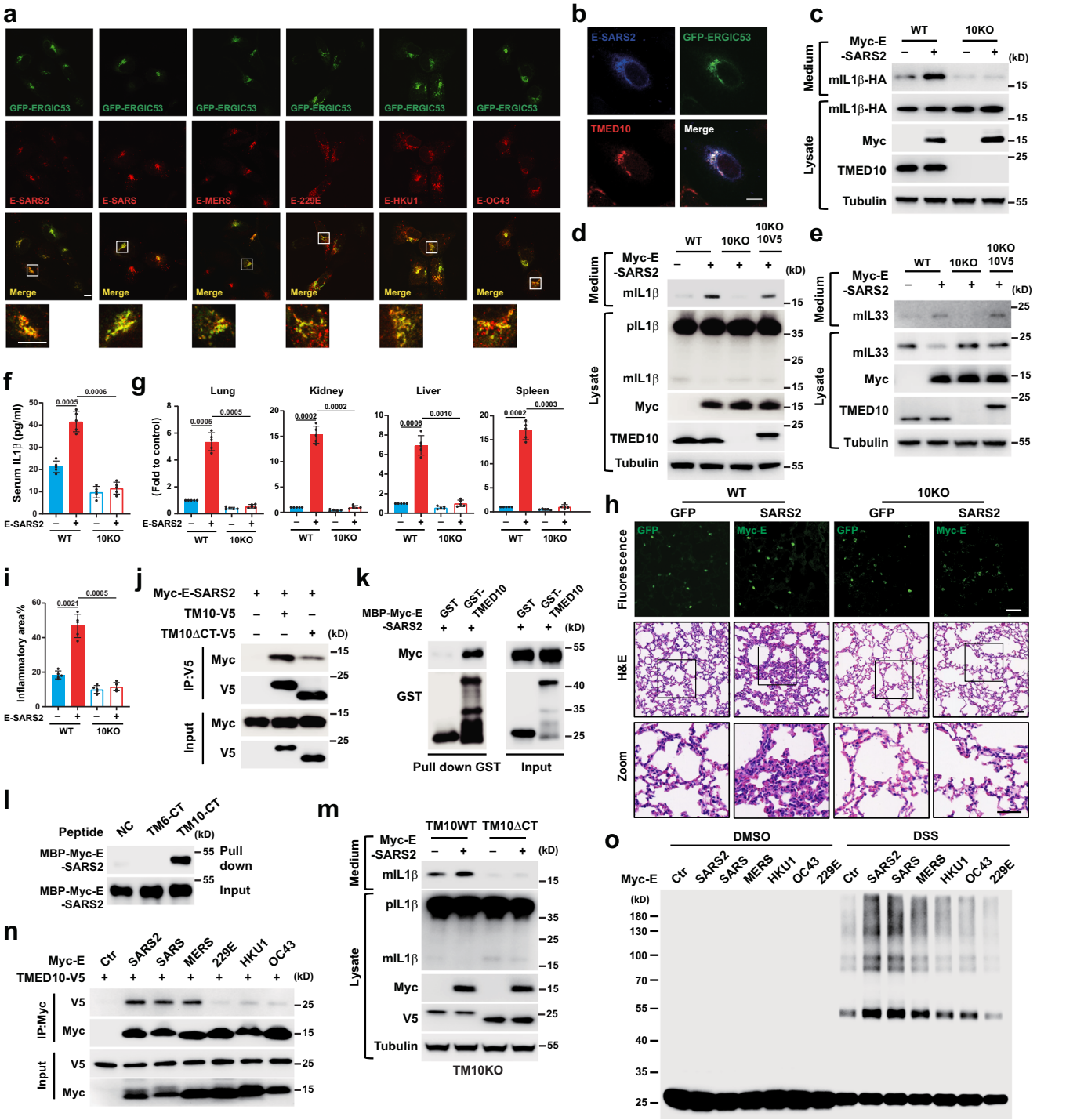

Fig. 2 | E-regulated UcPS is dependent on TMED10. a Immunofluorescence of U2OS expressing GFP-ERGIC53 and Myc-tagged E of indicated coronaviruses. **b** Immunofluorescence of U2OS expressing GFP-ERGIC53, TMED10-V5 and Myc-E-SARS2. **c** mIL1β-HA secretion in WT and TMED10-KO HEK293T cells transfected with mIL1β-HA alone or together expressed with or without Myc-E-SARS2. **d** mIL1β secretion in WT and TMED10-KO THP-1 cells expressed with or without Myc-E-SARS2, TMED10-V5 or both as indicated. **e** mIL33 secretion in WT or TMED10-KO BEAS-2B cells in the absence or presence of Myc-E-SARS2 or TMED10-V5 expression. **f**–**i** WT and TMED10KO mice injected with AAV-GFP or AAV-Myc-E-SARS2 were challenged with 15 mg/kg LPS for 15 h and euthanized. Expression of Myc-E-SARS2 or GFP in the lung was verified by IF (**h**, upper panel). Serum IL1β levels were determined by ELISA in (**f**). IL6 mRNA levels in indicated tissues were analyzed in (**g**). Lung inflammation was analyzed by H&E staining (**h**, middle and lower panel) and inflammatory area was quantified in (**i**). **j** Co-IP using HEK293T cells with Myc-E-SARS2 and TMED10-V5 or TMED10ΔCT-V5. **k** GST pull down analysis using GST, GST-TMED10, and MBP-Myc-E of SARS2 proteins. **l** Pull-down analysis using MBP-Myc-E of SARS2 protein and Ctrl, TMED6-CT or TMED10-CT peptides. **m** mIL1β secretion in TMED10-KO THP-1 cells transfected with or without Myc-E-SARS2 in the presence of TMED10-WT or TMED10ΔCT mutant. **n** Co-IP using HEK293T cells with TMED10-V5 and Myc-tagged E of indicated coronaviruses. **o** Crosslink assay performed using HEK293T cells expressing TMED10-V5 in the absence or presence of Myc-tagged E of indicated coronaviruses. WT, Wild type; 10KO, TMED10-KO; 10V5, TMED10-V5; TM10, TMED10; TM6, TMED6; DSS, disuccinimidyl suberate. Data are mean ± s.d. Statistical significance was assessed using one-way ANOVA ($n = 5$) followed by Tukey's multiple-comparison test. P values are indicated. Scale bars, 10 μm (**a**, **b**) and 50 μm (**k**). Source data are provided as a Source Data file.

https://doi.org/10.1038/s41467-024-52818-0

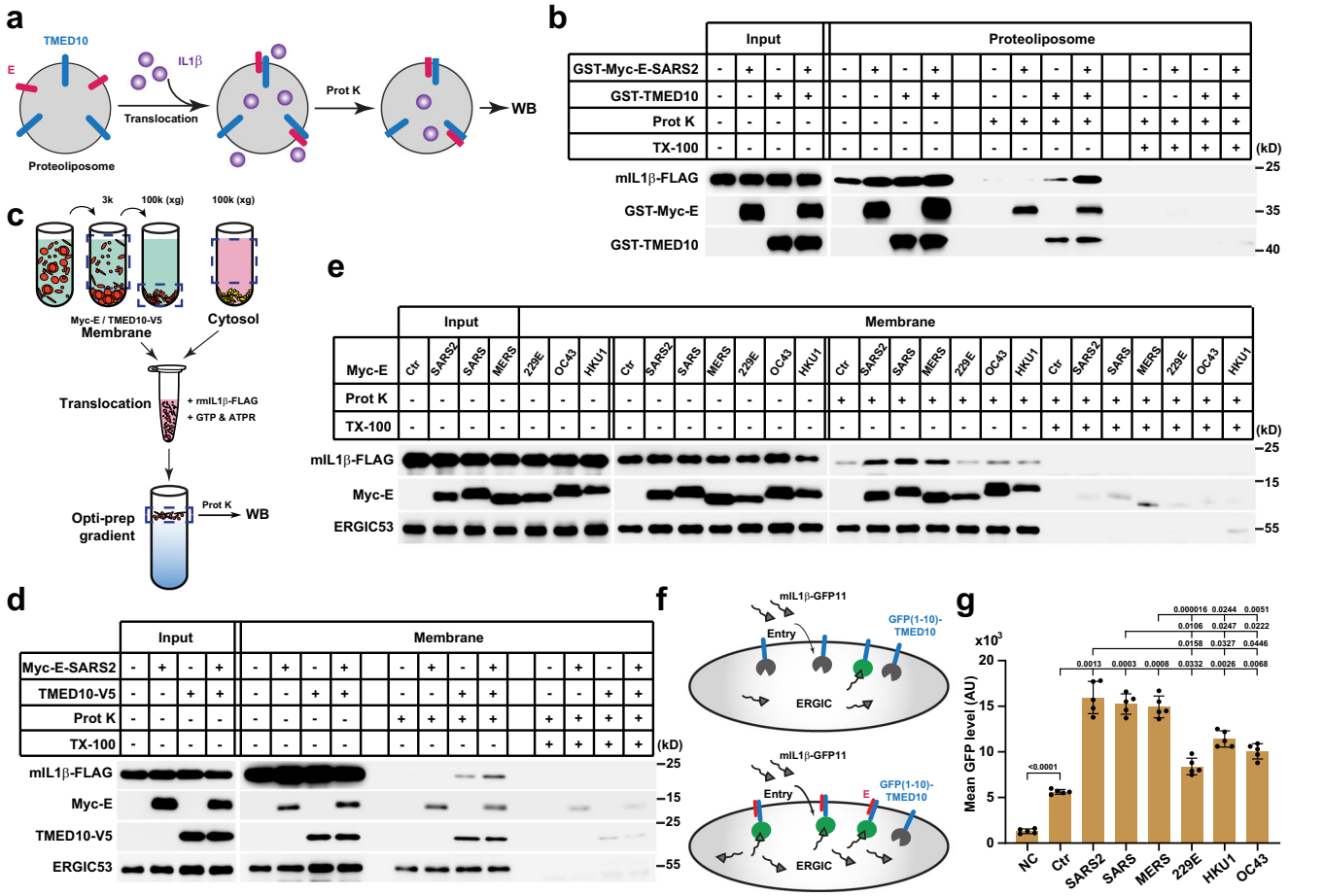

Fig. 3 | E protein facilitates the membrane translocation process of TMED10-mediated UcPS. a Diagram of in vitro translocation assay. In brief, proteoliposomes with GST-tagged Myc-E, TMED10 alone or both were incubated with recombinant mIL1β-FLAG protein at 30 °C for 1 h. Proteinase K digestion was performed to determine the amount of membrane-incorporated cargo. **b** In vitro membrane translocation of mIL1β-FLAG with control or GST-TMED10 proteoliposomes in the absence or presence of GST-Myc-E of SARS2. **c** Diagram of cell-free membrane translocation assay. In brief, membrane fraction collected from HEK293T cells expressing control (Ctrl), Myc-E-SARS2, TMED10-V5 or both after differential centrifugation was incubated with cytosol from HEK293T cells, recombinant mIL1β-FLAG plus GTP and ATPR for 1.5 h at 30 °C. After then, OptiPrep gradient ultracentrifugation was performed to remove the free proteins. Membrane floating on the top was collected and the translocated mIL1β was determined by proteinase K protection assay. **d** Cell-free membrane translocation of mIL1β-FLAG in the absence or presence of TMED10, Myc-E-SARS2 or both. The membrane fraction was collected from TMED10KO HEK293T cells. **e** Cell-free membrane translocation of mIL1β-FLAG in the absence or presence of Myc-tagged E of indicated coronaviruses. **f**, **g** Diagram of the GFP complementation assay (**f**). Cells expressing GFP (1–10)-TMED10 were transfected with negative control (NC) or mIL1β-GFP11 along without (Ctrl) or with Myc-tagged E of indicated coronaviruses. Complemented GFP signals were analyzed by FACS analysis and quantified in (**g**). Prot K, Protease K; TX-100, TritonX-100; ATPR, ATP regeneration system. Data are mean ± s.d. Statistical significance was assessed using one-way ANOVA ($n = 5$) followed by Tukey's multiple-comparison test. P values are indicated. Source data are provided as a Source Data file.

littermates (Fig. 2f–i). Collectively, these results provide strong evidence that E-SARS2 promotes the UcPS of mIL1β and other inflammatory factors through the THU pathway.

We sought to understand how the coronavirus E protein regulates UcPS through the THU. Our investigations revealed that the E-SARS2 protein exhibited a notable association with TMED10, as observed in co-immunoprecipitation (Co-IP) and GST-pull down experiments (Fig. 2j, k). Notably, E-SARS2 showed a reduced interaction with TMED10 lacking the C-terminal domain (TM10ΔCT mutant) (Fig. 2j). Furthermore, in a pull-down experiment, E-SARS2 was found to specifically interact with the C-terminal (CT) peptide of TMED10, but not with the CT of TMED6 (Fig. 2l). These findings strongly suggest a direct binding interaction between TMED10-CT and E-SARS2. In TMED10 knockout (TMED10KO) THP-1 cells, E-SARS2 effectively increased the secretion of IL1β when full-length TMED10 was reintroduced, but this rescue was not achieved when the TM10ΔCT variant was utilized (Fig. 2m). These findings underscore the indispensable role of the association between TMED10's C-terminal domain (TMED10-CT) and E-SARS2 in the regulation of E-SARS2-mediated UcPS.

Previous research from our group had indicated that TMED10 has the capacity to form oligomers in the presence of secretory cargo, potentially serving as a protein channel-like machinery responsible for the regulation of protein translocation[17]. Interestingly, E-SARS2 expression facilitates the self-association of TMED10 and boosts the formation of TMED10 oligomers in the presence and absence of IL1β, without affecting its interaction with another TMED family member, TMED2 (Supplementary Fig. 2c, d). This effect was contingent on the interaction between TMED10 and E-SARS2, as the oligomerization of the TM10ΔCT variant remained unaffected by E-SARS2 expression (Supplementary Fig. 2e). By using crosslinking, we were able to detect a ~ 38KDa band of E in the presence of TMED10, indicating to be a heterodimer of E and TMED10 (Supplementary Fig. 2f). However, we could barely detect the presence of E in high molecular weight bands (Supplementary Fig. 2f). The data suggest that E binds TMED10 which may make TMED10

monomer prone to form oligomers likely via enhancing cargo TMED10 binding as well as other unknown reasons that trigger conformation change of TMED10 favoring oligomerization. We also observed that the binding of the E protein with TMED10 does not inhibit but rather enhances the association between TMED10 and IL1β (Supplementary Fig. 2g). This could be due to the E protein promoting the formation of TMED10 homo-oligomers, which increases the number of cargo binding sites through multiple C-terminal tails in the oligomer.

Crucially, Es-SSC exhibited a stronger association with TMED10 compared to Es-MSC (Fig. 2n), and consequently more effectively increased TMED10 oligomerization (Fig. 2o). These results suggest that TMED10 may represent a host target for Es-SSC in the facilitation of UcPS for inflammatory factors.

E facilitates cargo membrane translocation

In THU, TMED10 serves the essential role of facilitating the translocation of cargoes into the ERGIC[17]. This process involves ushering leaderless UcPS cargo into the vesicle trafficking system to initiate the UcPS pathway within the cell. To assess whether the E protein supports the entry of secretory cargo into vesicles, an established in vitro membrane translocation assay was conducted (Fig. 3a). As previously demonstrated, the presence of TMED10 on the liposome effectively promoted the translocation of mIL1β into the liposome, as indicated by its protection from proteinase K digestion. Notably, E-SARS2 alone in the liposome exhibited limited cargo translocation ability, but in combination with TMED10, it significantly augmented TMED10-facilitated translocation (Fig. 3b, Supplementary Fig. 3a). A comparable enhancement of TMED10-mediated translocation was also observed with E-SARS (Supplementary Fig. 3a, b). These findings substantiate that both E-SARS2 and E-SARS directly enhance the translocation of UcPS cargo into vesicles via TMED10.

Given the unavailability of E protein from other coronaviruses, a cell-free UcPS cargo translocation assay was developed utilizing membrane fractions from cells expressing various E proteins (Fig. 3c). Similar to the liposome assay, E-SARS2 elevated mIL1β translocation in the presence of TMED10 (Fig. 3d). Additionally, Es-SSC promoted mIL1β translocation, whereas Es-MSC exhibited a lesser impact on mIL1β translocation (Fig. 3e). To further corroborate the differential effects of E proteins on cargo entry into vesicles, a GFP complementation assay was employed, as previously established[17], to assess UcPS cargo translocation into the ERGIC (Fig. 3f). In this assay, a GFP1-10 fragment was fused to the luminal segment of TMED10 to evaluate the translocation of GFP11-tagged mIL1β into the ERGIC lumen, where GFP complementation occurs. Once again, Es-SSC, rather than Es-MSC, was found to enhance mIL1β entry into the ERGIC (Fig. 3g, Supplementary Fig. 3c). These results collectively suggest that Es-SSC augments the UcPS of inflammatory factors by promoting cargo translocation within THU.

An SS/DS motif in Es-SSC determines their effect on TMED10-mediated UcPS

Sequence alignment revealed the presence of an SS/DS motif in Es-SSC but its absence in Es-MSC (Fig. 4a). The alteration of the SS/DS motif minimally impacted the ERGIC localization of Es-SSC (Supplementary Fig. 4a). However, this mutation significantly compromised Es-SSC's capacity to enhance mIL1β secretion in both non-inflammatory and inflammatory cells (Fig. 4b, c), hindered its association with TMED10, and its ability to facilitate cargo translocation (E-SARS2) (Fig. 4d, e). This suggests that the SS/DS motif is essential for Es-SSC to augment the THU pathway.

Conversely, the introduction of the SS motif into Es-MSC increased their interaction with TMED10, regulated secretion, and enhanced cargo translocation (Fig. 4f–k). It is conceivable that pathogenic coronavirus E proteins may possess an SS/DS motif that plays a crucial role in promoting UcPS of inflammatory factors.

E-TMED10 interaction is required for E-induced inflammation

The presented data suggests that the interaction between E and TMED10 initiates TMED10 oligomerization and cargo translocation, resulting in the release of various inflammatory factors through the THU pathway. Our objective was to investigate whether blocking the E-TMED10 complex could mitigate inflammation induced by E expression. E is a small protein characterized by a luminal N-terminal domain, a transmembrane domain, and a C-terminal (CT) cytosolic domain (Fig. 5a)[31]. The association of E-SARS2 with TMED10-CT suggests a potential interaction between the cytosolic portion of E-SARS2 and the CT of TMED10. To disrupt the E-TMED10 interaction, we overexpressed TMED10-CT or E-SARS2-CT. Remarkably, the expression of green fluorescent protein-tagged E-SARS2-CT (GFP-ECT), as opposed to TMED10-CT expression, effectively impeded the E-TMED10 interaction (Fig. 5b, Supplementary Fig. 4b). Consistently, the expression of GFP-ECT demonstrated a dose-dependent inhibition of E-SARS2 induced mIL1β secretion in both HEK293T cells and THP-1 cells (Fig. 5c, d). In experiments involving crosslinking and translocation, GFP-ECT reduced E-facilitated TMED10 oligomerization and the translocation of mIL1β into the membrane fraction (Fig. 5e, f). In a mouse model, the expression of GFP-ECT resulted in diminished inflammation, as indicated by reduced levels of IL1β in the serum and correspondingly reduced production of IL6 in the lung, kidney, liver, and spleen (Fig. 5g–j). These findings emphasize the essential role of E-TMED10 interaction in facilitating E-SARS2-induced release of inflammatory factors through the THU pathway.

Progesterone and its analogs inhibit E-induced inflammatory factor release

Our findings suggest that the E protein's induction of inflammatory factor release via the THU pathway may contribute to the development of severe inflammation in SARS-CoV-2 and other coronaviruses, leading to severe symptoms. Subsequently, we conducted a search for inhibitors against E-induced UcPS, which could serve as a potential target for mitigating severe inflammation resulting from coronavirus infections. To facilitate this investigation, we established a rapid secretion analysis assay using complementary NanoLuc luciferase[53]. This assay was then combined with high-throughput compound screening to identify chemical modulators of E-mediated UcPS (Fig. 6a).

Out of approximately 2500 FDA-approved drugs, we discovered that progesterone and some of its analogs exhibited strong inhibitory effects on E-stimulated UcPS (Fig. 6b, c). Both progesterone and its analog Ulipristal acetate (UPA) effectively suppressed the release of IL1β induced by E-SARS2-SSC in THP-1 cells (Fig. 6d, e). Similar to the ECT-peptide, progesterone and UPA blocked the interaction between E and TMED10, inhibited E-induced TMED10 oligomer formation, and prevented E-enhanced mIL1β translocation (Fig. 6f–h). These findings suggest that these two drugs may function through a mechanism similar to ECT. In a mouse experiment, UPA reduced lung inflammation caused by the expression of E-SARS2 (Fig. 6i–l). Consequently, we conclude that progesterone and its analogs inhibit E-induced UcPS by disrupting the interaction between E and TMED10.

To further elucidate the structural features necessary for the inhibitory function of progesterone and its analogs in regulating UcPS mediated by TMED10, we evaluated the effects of 23 progesterone analogs on E-enhanced mIL1β secretion (Fig. 6m, Supplementary Data 1). Interestingly, we observed that modifications at position 11 on the steroid core of progesterone analogs, such as the introduction of a carbonyl or hydroxyl group, largely abolished their inhibitory effects (Fig. 6m). However, the presence of an N, N-dimethylaniline modification at position 11, as seen in UPA, did not diminish the inhibitory effect (Fig. 6m). Furthermore, we observed various modifications at position 17 within the progesterone analogs, but these modifications did not significantly impact the activity of these compounds in regulating E-enhanced UcPS in the secretion assay (Fig. 6n).

https://doi.org/10.1038/s41467-024-52818-0

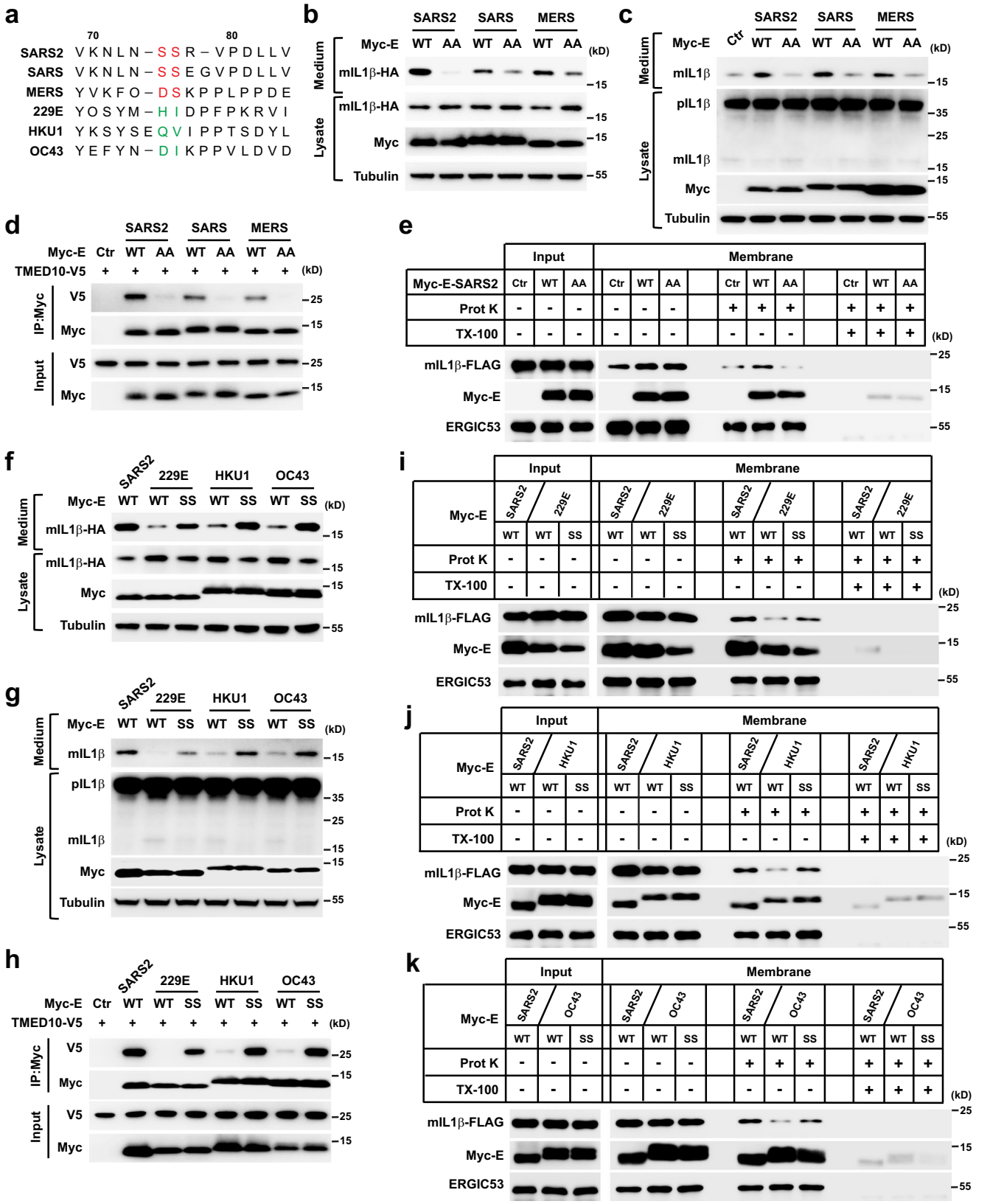

TMED10 controls MHV-induced UcPS of inflammatory factors

In order to investigate the role of TMED10-regulated UcPS in the release of inflammatory factors during coronavirus infection, we established an infection model using Murine Hepatitis Virus (MHV) in HEK293T cells and bone marrow-derived macrophages (BMDMs)[54]. Similar to the effects observed with E protein expression, MHV infection elicited a dose-dependent release of mIL1β in HEK293T cells expressing the MHV receptor mCC1a (Fig. 7a). Importantly, we observed that Caspase-3 cleavage, indicative of cell death, did not increase during MHV infection, implying that mIL1β release was more likely attributed to UcPS rather than cell death (Fig. 7a).

https://doi.org/10.1038/s41467-024-52818-0

Fig. 4 | An SS/DS motif in Es-SSC regulates TMED10-mediated UcPS. a C-terminal partial amino acid sequence alignment of indicated coronaviruses E protein. SS/DS residues of Es-SSC are marked in red. The alternative residues of Es-MSC are marked in green. **b** mIL1β-HA secretion in HEK293T cells transfected with Myc-tagged E WT or AA mutant of indicated severe symptom coronaviruses. **c** mIL1β secretion in THP-1 cells expressed with Myc-tagged E WT or AA mutant of indicated severe symptom coronaviruses. **d** Co-IP using HEK293T cells with TMED10-V5 and Myc-E WT or AA mutant of indicated severe symptom coronaviruses. **e** Cell-free membrane translocation of mIL1β-FLAG in the absence or presence of Myc-E WT or AA mutant of SARS2. **f** mIL1β-HA secretion in HEK293T cells transfected with Myc-tagged E-SARS2, Myc-tagged E WT or SS mutant of indicated mild symptom coronaviruses. **g** mIL1β secretion in THP-1 cells expressed with Myc-tagged E-SARS2, Myc-tagged E WT or SS mutant of indicated mild symptom coronaviruses. **h** Co-IP using HEK293T cells with TMED10-V5 and Myc-tagged E-SARS2, Myc-tagged E WT or SS mutant of indicated mild symptom coronaviruses. **i**–**k** Cell-free membrane translocation of mIL1β-FLAG in the absence or presence of Myc-tagged E-SARS2, Myc-tagged E WT or SS mutant of indicated mild symptom coronaviruses. Prot K, Protease K; TX-100, TritonX-100. Source data are provided as a Source Data file.

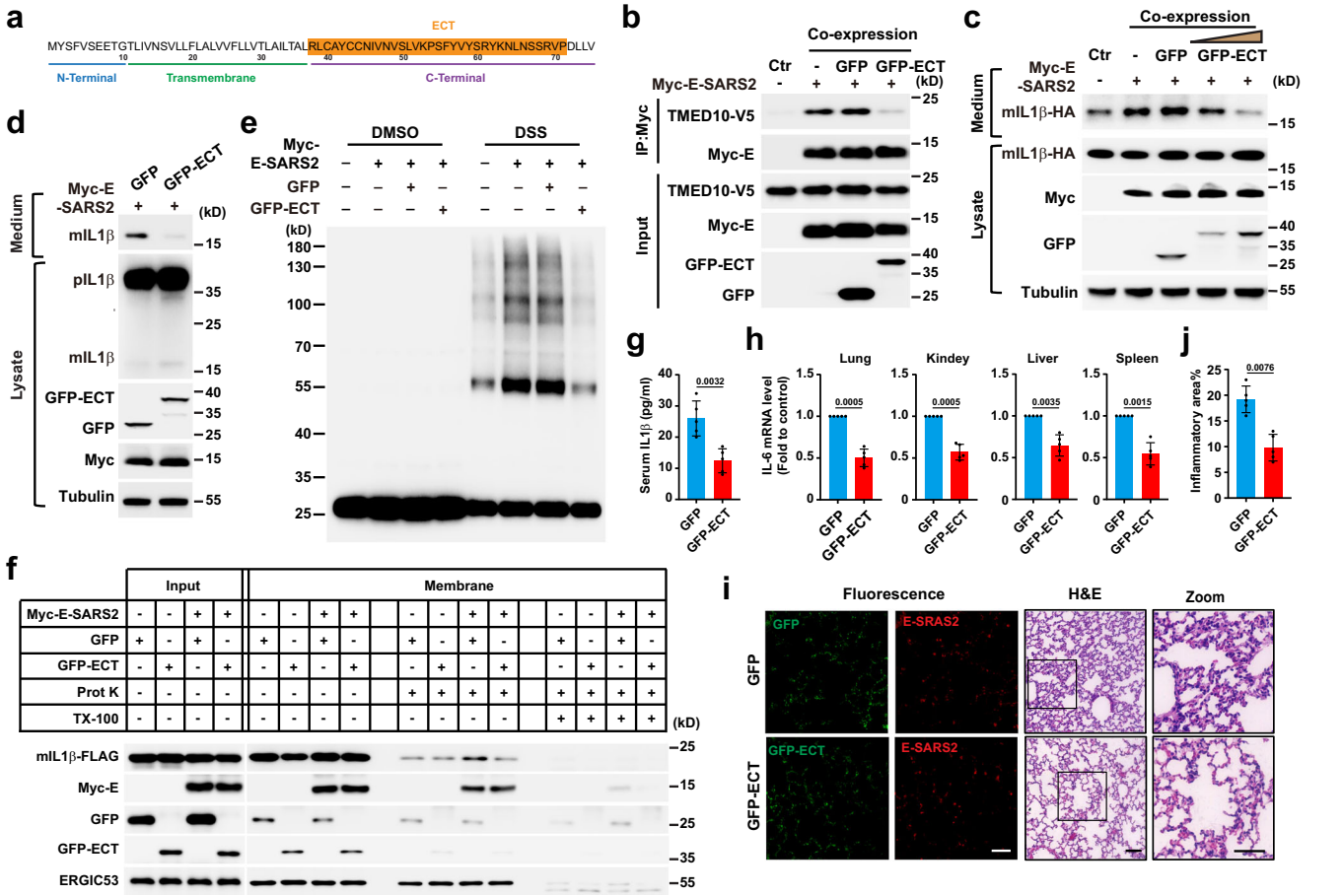

Fig. 5 | E-TMED10 interaction is required for E-induced inflammation. a Amino acid sequence and domains of the SARS2-E protein. The C-terminal region of SARS2-E (ECT) used to block E-TMED10 interaction is highlighted in orange. **b** Co-IP using HEK293T cells with TMED10-V5 and Myc-tagged E-SARS2 in the absence or presence of GFP or GFP-tagged CT of E-SARS2 (GFP-ECT). **c** mIL1β-HA secretion in HEK293T cells transfected with or without Myc-tagged E-SARS2, or in the absence or presence of GFP or increasing amount of GFP-ECT. **d** THP-1 cells were expressed with GFP or GFP-ECT followed by differentiation and mIL1β secretion determination. **e** Crosslink assay performed using HEK293T cells expressing TMED10-V5 in the absence or presence of Myc-E-SARS2, GFP or GFP-ECT as indicated. **f** Cell-free membrane translocation of mIL1β-FLAG in the absence or presence of Myc-E-SARS2 and cytosol in the presence of GFP or GFP-ECT as indicated. **g**–**j** C57BL/6 mice co-injected with AAV-Myc-E-SARS2 and AAV-GFP or AAV-GFP-ECT were challenged with LPS and euthanized. Expression of Myc-E-SARS2, GFP, GFP-ECT in the lung were verified by IF (**i**, left panel). Serum IL1β levels were determined by ELISA (**g**). IL6 mRNA levels in indicated tissues were analyzed in (**h**). Lung inflammation was analyzed by H&E staining (**i**, right panel) and inflammatory area was quantified in (**j**). Prot K, Protease K; TX-100, TritonX-100. Data are mean ± s.d. Statistical significance was assessed using two-tailed t test ($n = 5$). P values are indicated. Scale bars, 50 μm. Source data are provided as a Source Data file.

In the case of BMDMs, the release of mIL1β induced by MHV infection was found to be dependent on TMED10 rather than GSDMD (Fig. 7b, c), underscoring the involvement of the THU pathway. Furthermore, the expression of ECT or the administration of progesterone (or UPA) effectively blocked the MHV infection-induced mIL1β secretion and the interaction between E-MHV and TMED10 (Fig. 7d–g), highlighting the significance of the E-TMED10 interaction in this process.

In a murine lung infection model using IFNAR-KO mice[55,56], MHV infection resulted in severe lung infection, characterized by the release of mIL1β, immune cell infiltration, and the activation of IL6 production in multiple organs (Fig. 7h–o). These effects mirrored those seen with E protein expression in the presence of mild LPS challenges. Significantly, the expression of ECT or treatment with progesterone
(or UPA) mitigated the inflammation following MHV infection, further substantiating the role of these interventions in modulating the inflammatory response (Fig. 7h–o). The mitigating effect of progesterone on inflammation induced by coronavirus was reported in two other studies, aligning with our current findings[57,58].

https://doi.org/10.1038/s41467-024-52818-0

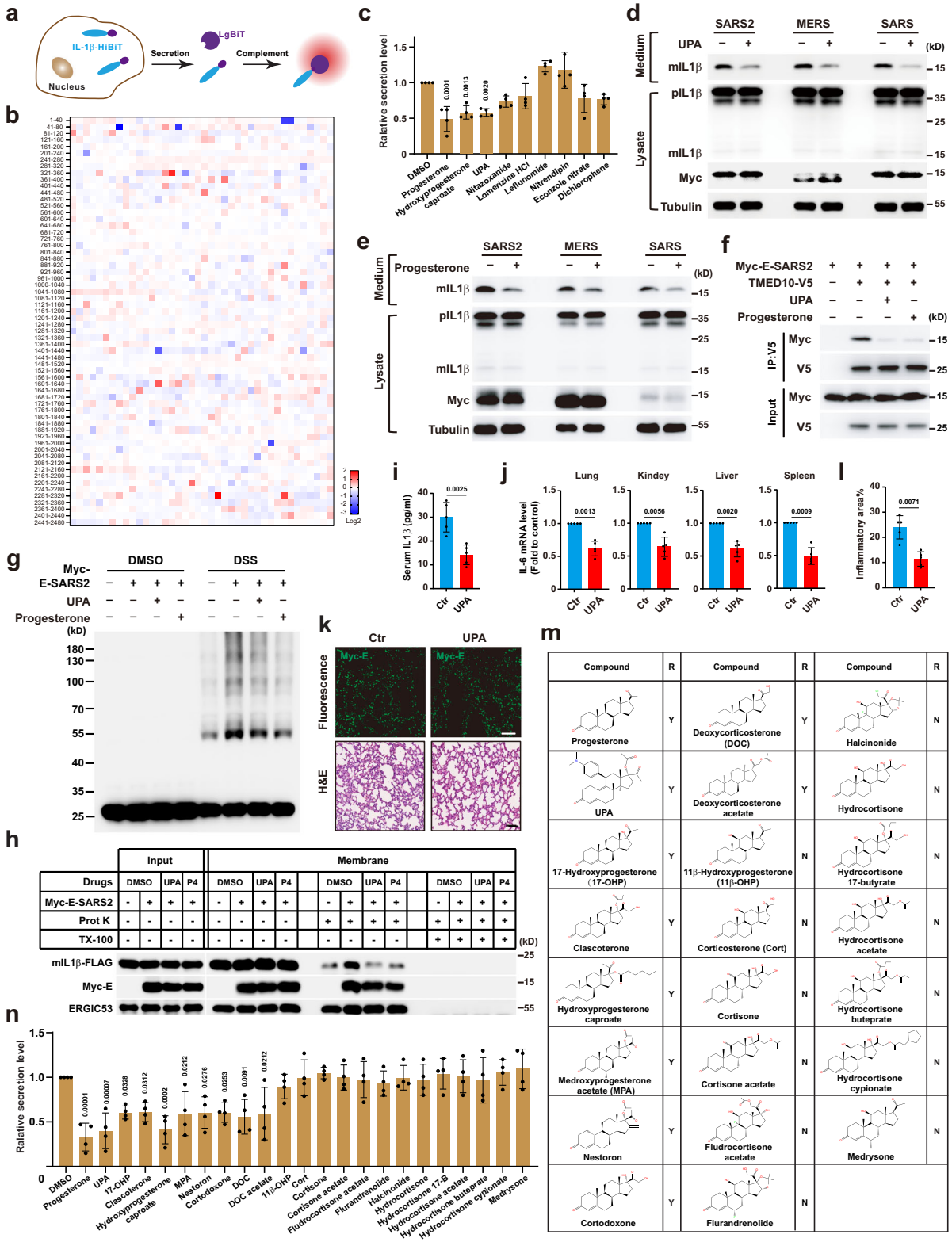

Discussion

In summary, our research uncovers a crucial molecular interaction, namely the E-TMED10 interaction, which triggers the THU-mediated release of inflammatory factors and consequently results in severe inflammation during coronavirus infections. Our findings from cellular, molecular, and murine experiments, strongly underscores the potential of targeting the E-TMED10 interaction as a therapeutic strategy to combat the lethal cytokine storm induced by SARS-CoV-2 and other highly virulent coronaviruses.

The coronavirus E protein has garnered attention as a key structural component implicated in various stages of the virus lifecycle and directly linked to pathogenic processes[59,60]. Multiple investigations have highlighted its ability to form ion channels, leading to cell death, particularly noteworthy in inflammatory cells where E-induced ion

Fig. 6 | Progesterone and UPA are inhibitors of E-induced secretion and inflammation. a Diagram of the high-throughput compound screening system based on cargo secretion analysis by complementary NanoLuc luciferase. **b** Heatmap showing the average mIL1β-HiBiT secretion levels from two independent experiments by each compound normalized to control. The numbers on the left side of heatmap show the serial numbers of compounds in each row. The heatmap shows the log2 value. **c** Quantification of relative mIL1β secretion levels in HEK293T cells in the presence of 10 μM indicated compounds. **d**–**e** mIL1β secretion in THP-1 cells expressed with Myc-tagged E of indicated coronaviruses in the presence of 10 μM UPA (**d**) or Progesterone (**e**) for 4 h. **f** Co-IP using HEK293T cells with TMED10-V5 and Myc-E-SARS2 in the absence or presence of 10 μM UPA or Progesterone. **g** Crosslink assay performed using HEK293T cells expressing TMED10-V5 without or with Myc-E-SARS2 in the absence or presence of 10 μM UPA or Progesterone. **h** Cell-free membrane translocation of mIL1β-FLAG in the absence or presence of Myc-E-SARS2, UPA or Progesterone (P4) as indicated. **i**–**k** C57BL/6 mice infected with AAV-Myc-E-SARS2 were intraperitoneal injected with or without UPA (1 mg/kg) followed by challenge with LPS and euthanized. Expression of Myc-E-SARS2 in the lung was verified by immunofluorescence (**k**, upper panel). Serum IL1β levels were determined by ELISA in (**i**). IL6 mRNA levels in indicated tissues were analyzed in (**j**). Lung inflammation was analyzed by H&E staining (**k**, lower panel) and inflammatory area was quantified in (**l**). **m** Chemical structure and names of Progesterone and its analogs with (Y) or without (N) inhibitory effect on mIL1β secretion in HEK293T cells shown in (**n**). **n** Quantification of relative mIL1β secretion levels in HEK293T cells in the absence or presence of compounds in (**m**). DSS, disuccinimidyl suberate; Prot K, Protease K; TX-100, TritonX-100. Data are mean ± s.d. Statistical significance was assessed one-way ANOVA (n = 4) followed by Dunnett's multiple-comparison test (**c, n**), two-tailed t test ($n = 5$) (**i, j, l**). P values are indicated. Scale bars, 50 μm. Source data are provided as a Source Data file.

channels activate the inflammasome, prompting pyroptosis[5,44–46]. Furthermore, surface-localized E proteins of SARS-CoV-2 can activate TLR2, eliciting an inflammatory response[61]. Additionally, E proteins can interact with cell junction proteins, disrupting epithelial cell junctions and causing tissue leakage and damage[62,63].

Consistent with these findings, our research supports the concept that the E protein serves as a pathogenic factor contributing to tissue damage and inflammation. Furthermore, our investigation sheds light on the differential host inflammatory responses triggered by severe and mild coronaviruses. At the molecular level, we propose a model in which E proteins from severe-symptom-causing coronaviruses, including SARS-CoV-2, SARS and MERS, interact with TMED10 to activate THU-mediated release of inflammatory cytokines (Fig. 7p). Mechanistically, a specific SS/DS motif present in severe coronaviruses, absent in mild counterparts, enhances interaction with TMED10, promoting its oligomerization—a critical step in the translocation process essential for the UcPS of various inflammatory factors. Furthermore, it is noteworthy that coronavirus E proteins can form ion channels, capable of triggering inflammasome activation[5,44,45]. In this context, the pro-inflammatory role of E proteins aligns with their facilitation of inflammatory factor release, collectively contributing to the extensive release of such factors as a risk factor for the development of severe symptoms in coronavirus infections.

Recent studies have demonstrated that SARS-CoV-2 ORF8, a protein equipped with a signal peptide, can be secreted through both conventional and unconventional pathways[64,65]. Notably, the unconventional secretion pathway allows ORF8 to evade glycosylation, resulting in the release of an unglycosylated form of the protein[64]. This unglycosylated ORF8 has been implicated in the induction of pro-inflammatory cytokines by binding to the IL17RA receptor[64,66]. Investigating the regulatory mechanisms that govern these distinct ORF8 secretion pathways is of significant scientific interest. It remains to be elucidated whether the unconventional secretion of ORF8 is regulated through TMED10-mediated translocation.

A characteristic of viral infection at the cellular level involves the manipulation of the host cellular machinery, leading to disruptions in cellular function that can potentially be targeted for antiviral interventions. In the context of SARS-CoV-2 infection, the virus exploits the host autophagy-lysosome system for release through ORF3a, repurposing degradative autophagy for secretion[54,67]. Additionally, Nsp3 and Nsp4 collaborate with host factors VMP1 and TMEM41B to modify the endoplasmic reticulum (ER) membrane, forming double-membrane vesicles crucial for virus replication[68–70]. Our research adds to this understanding by demonstrating that the E protein of various coronaviruses interacts with TMED10, triggering host inflammation, and suggests that disrupting the E-TMED10 interaction could be a viable anti-inflammatory strategy.

Notably, we discovered that progesterone analogs inhibit the E-TMED10 interaction, offering protection against hyperinflammatory damage induced by both E protein expression and coronavirus infection. This finding provides insight into the previously unexplained gender differences observed in COVID-19 severity, where males exhibit higher severity and fatality rates compared to females[71]. Given that the E-TMED10 interaction represents a common target for inflammation modulation among severe coronaviruses, progesterone analogs may serve as promising lead compounds for the development of novel anti-inflammatory drugs against current COVID 19 and future pandemics caused by new deadly coronaviruses. It is noteworthy that while our findings suggest the inhibition of the E-TMED10 interaction as a potential target for progesterone analogs, it remains uncertain whether other unidentified targets exist in the case of proinflammatory factor UcPS. Our study on how viral factors influence the release of non-classical inflammatory cytokines has opened up new avenues of investigation into how pathogen-host interactions lead to inflammation, which can guide the study of inflammation caused by other viruses, such as influenza, HBV, and Zika.

Methods

This study complied with all of the relevant ethical regulations. All mice experiments were approved by the Institutional Animal Care and Use Committees at Tsinghua University (permission number: 22-ZM5).

Plasmids and cells

The mature form of IL1 family proteins (IL1α, IL1β, IL18, IL33, IL36α), IL6, TMED10-V5, TMED10ΔCT-V5, HA-TMED10, GFP (1-10)-TMED10-V5, mIL1β-FLAG-GFP11 plasmids and mIL1β, TMED10 protein purification plasmids were generated in our previous work[17]. FLAG-tagged expression plasmids of SARS2 proteins (E, M, S, N, ORF3a, ORF6, ORF7b, and ORF8) were described as previously[72]. E-SARS2 expression plasmids with or without an N-terminal Myc tag were PCR amplified from the template and inserted into the FUGW vector. Expression plasmids of E proteins of SARS, MERS, 229E, HKU1, OC43 and MHV were generated by DNA synthesize followed by inserting into the FUGW vector with a Myc tag at the N terminus. Mutants of E proteins were constructed by mutagenesis PCR. GFP-ECT was generated by PCR amplification from 38-71aa of E-SARS2 C-terminal and inserted into the FUGW vector with a GFP tag at the N terminus. Myc-E-SARS2, Myc-E-SARS were also inserted into pGEX4T1 or pET28a vector with a GST or MBP tag for protein purification.

HEK293T (from Dr. Randy Schekman), TMED10-KO HEK293T (from our laboratory), U2OS (from Dr. Randy Schekman), BEAS-2B (from Dr. Yu Rao) and 17Cl-1 (from Dr. Fuping You) cells were cultured in Dulbecco's modified Eagle's medium supplemented with 10% fetal bovine serum (FBS) and 1% Pen-Strep. THP1 (from Dr. Gong Cheng), TMED10-KO (from our laboratory) and GSDMD-KO THP1 (from our laboratory) cells were maintained in RPMI-1640 medium supplemented with 10% FBS and 1% Pen-Strep. The cells were cultured at 37 °C with 5% CO_2. Bone marrow-derived macrophages (BMDMs) were isolated from 6-week-old male C57BL/6 mice and differentiated using standard protocols[73].

https://doi.org/10.1038/s41467-024-52818-0

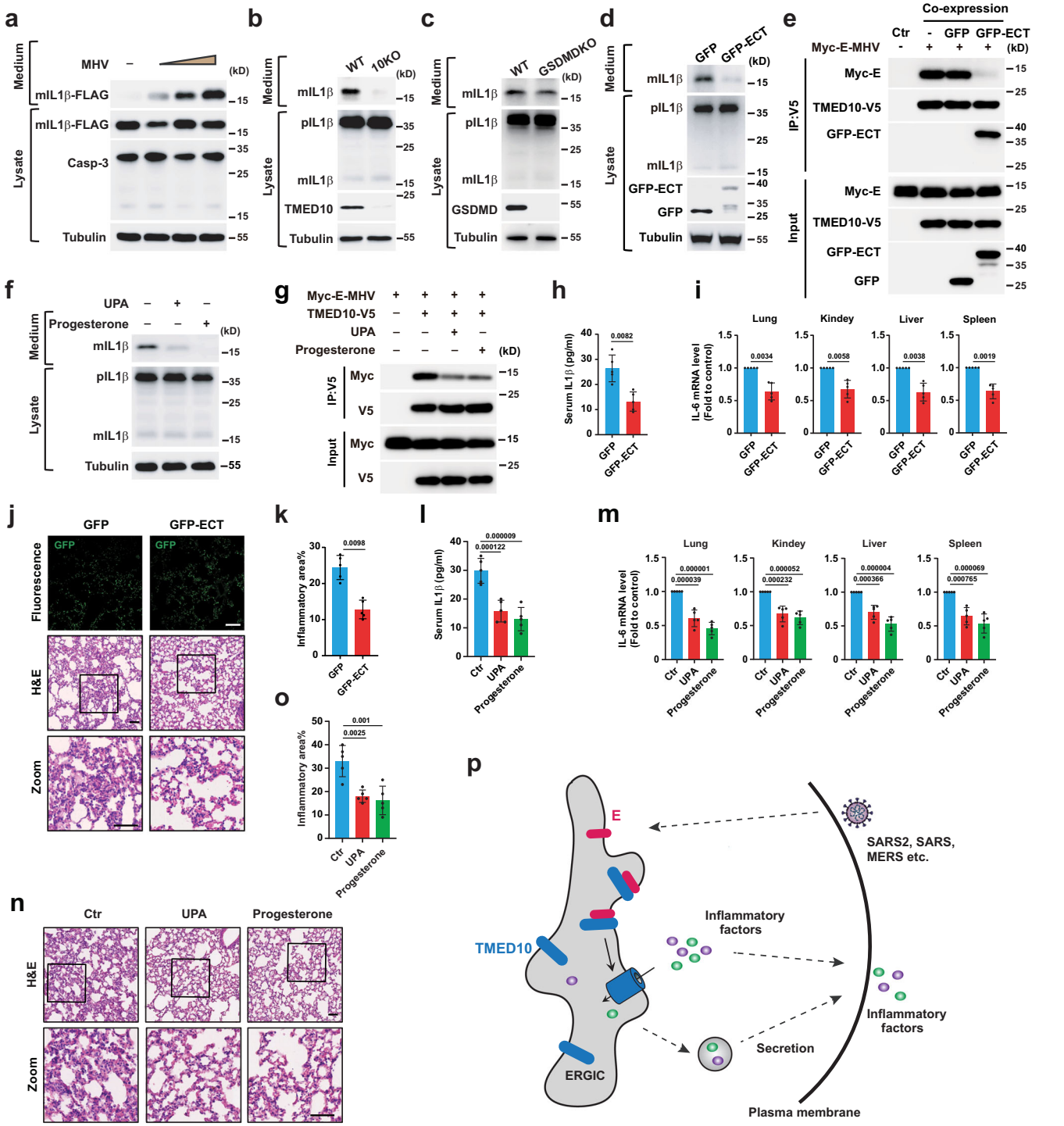

Fig. 7 | E-regulates UcPS and inflammation in MHV-infected mice. a mIL1β-FLAG secretion and Caspase-3 cleavage in HEK293T-mCC1a cells infected without or with MHV-A59 for 36 h at a MOI of 0.005, 0.05 and 0.5. **b**, **c** mIL1β secretion in MHV-A59 (MOI 0.1, 36 h) infected BMDMs from WT, TMED10 KO (**b**) or GSDMD KO (**c**) mice. **d** mIL1β secretion in MHV-A59 (MOI 0.1, 36 h) infected BMDMs in the presence of GFP or GFP-ECT. **e** Co-IP using HEK293T cells with TMED10-V5 and Myc-tagged E-MHV in the absence or presence of GFP or GFP-ECT. **f** mIL1β secretion in MHV-A59 (MOI 0.1, 36 h) infected BMDMs in the absence or presence of 10 μM UPA or Progesterone. **g** Co-IP using HEK293T cells with TMED10-V5 and Myc-E-MHV in the absence or presence of 10 μM UPA or Progesterone. **h**–**k**, IFNAR-KO mice injected with AAV-GFP or AAV-GFP-ECT were infected with MHV-A59 for 4 days and euthanized. Expression of GFP or GFP-ECT in the lung was verified by IF (**j**, upper panel). Serum IL1β levels were determined by ELISA (**h**). IL6 mRNA levels in indicated tissues was analyzed (**i**). Lung inflammation was analyzed by H&E staining (**j**, middle and lower panel) and inflammatory area was quantified (**k**). **l**–**o** IFNAR-KO mice infected with MHV-A59 were intraperitoneal injected with DMSO, 1 mg/kg UPA or Progesterone and euthanized. Serum IL1β levels were determined by ELISA (**l**). IL6 mRNA levels in indicated tissues were analyzed in (**m**). Lung inflammation was analyzed by H&E staining (**n**) and inflammatory area was quantified in (**o**). **p** A model for E-regulated UcPS. In brief, E proteins of the severe symptom coronaviruses (SARS, SARS2 and MERS) interact with TMED10 to activate the THU (TMED10-channel unconventional protein secretion)-mediated release of inflammatory cytokines. Data are mean ± s.d. Statistical significance was assessed using two-tailed t test ($n = 5$) (**h, i, k**), one-way ANOVA ($n = 5$) followed by Tukey's multiple-comparison test (**l, m, o**). P values are indicated. Scale bars, 50μm. Source data are provided as a Source Data file.

Reagents and antibodies

The reagents used in this study were purchased from the following sources: DSS (Thermo, 21655), GTP (Roche, 11140957001), ATP (Sigma, A2383), Creatine phosphate (Calbiochem, 2380), Creatine Kinase (Roche, 10127566001), Proteinase K (ABCone, P78893), Phenylmethylsulfonyl fluoride (PMSF) (Beyotime, ST505), Opti-Prep (Serumwerk Bernburg AG, 1893), Protease inhibitor cocktail (Roche, 11697498001), Phosphotase inhibitors (Roche, 4906845001), LPS (Sigma, L2880), Mouse IL-1 beta Uncoated ELISA Kit (Thermo, 88-7013-22), anti-V5 agarose (Sigma, A7345), anti-Myc agarose (Thermo, 20168). Progesterone (S1705), Nitazoxanide (S1627), Leflunomide (S1247), Nitrendipine (S2491), Lomerizine 2HCl (S4084), Econazole Nitrate (S2535), Hexachlorophene (S4632), Hydroxyprogesterone caproate (S4674), Dichlorophen (S5724) all purchased from Selleck, Ulipristal acetate (MEC, HY-N0437) and Progesterone analogs all purchased from MCE.

The antibodies used in this study were obtained from the indicated source: rabbit anti-HA(CST, 3724; WB, 1:5,000), mouse anti-FLAG (Sigma, F3165; WB, 1:5,000), mouse anti-β-tubulin (ZENBIO, 200608; WB, 1:5,000), mouse anti-Myc (CST, 2276; WB, 1:5,000; IF, 1:500), goat anti-IL1β (R&D Systems, BAF401; WB, 1:2,000), rabbit anti-IL1β (Abcam, ab9722; WB, 1:5,000), rabbit anti-GSDMD (CST, 39754; WB: 1:2,000), rabbit anti-IL33 (Proteintech, 12372-1-AP; WB, 1:1,000), rabbit anti-V5 (CST, 13202; WB, 1:1,000; IF, 1:500), mouse anti-V5 (CST, 80076; WB, 1:5,000), rabbit anti-TMED10 (Proteintech, 15199-1-AP; WB, 1:3,000), rabbit anti-TMED2 (Proteintech, 11981-1-AP; WB, 1:3,000), mouse anti-GST (CST, 2624; WB, 1:5,000), rabbit anti-ERGIC53 (Sigma, E1031; WB, 1:2,000), rabbit anti-GFP (CST, 2956; WB, 1:5,000), rabbit anti-Caspase3 (CST, 9662; WB: 1:2,000), rabbit anti-RPN1 (raised against C-terminal peptides corresponding to human protein residues 588–605 and mouse protein residues 576–605; from R. Schekman; WB, 1:5,000) and rabbit anti-E-SARS2 (raised against C-terminal peptides corresponding to the last 25 residues of E-SARS2 protein; purified by ABclonal; WB, 1:1,000). Goat anti-rabbit IgG Alexa Fluor 568 (Invitrogen, A-11011), goat anti-mouse IgG Alexa Fluor 568 (Invitrogen, A-11004) and goat anti-mouse IgG Alexa Fluor Plus 647 (Invitrogen, A32733) were used at a dilution of 1:500 for IF.

Mice

Mice were housed in ventilated cages kept at relatively stable temperature and humidity (20 °C-26 °C, 40%-70%) and light regulated room (12 h light/12 h dark) in a SPF facility and received food and water ad libitum. C57BL/6 J mice were purchased from the Laboratory Animal Resources Center at Tsinghua University. TMED10 fl/fl mice (C57BL/6) were created by GemPharmatech Co. Ltd, China. TMED10 inducible whole body knockout mice were generated via crossbreeding of TMED10 fl/fl with Cre-ERT mice (from Dr. Xiaoyu Hu). 8-week-old male mice were intraperitoneally injected with tamoxifen (80 mg/kg) or corn oil for five continuous days. After the final tamoxifen injection, the mice were fed normally for an additional week before being utilized in an AAV infection experiment.

Transfection, lentiviral transduction and secretion determination

Transfection of DNA constructs into cells was performed using PEI (Polysciences, 23966) for HEK293T and X-tremeGENE HP (Roche, 6366244001) for U2OS according to the manufacturer's protocols. Lentiviral transduction was used to express TMED10, E, and mutants, GFP and GFP-ECT in THP-1, BEAS-2B or BMDMs. pLX304 plasmids containing the TMED10-V5 or FUGW plasmids containing Myc-E of indicated coronavirus together with pMD2.G and psPAX2 were transfected into HEK293T cells to produce lentiviral particles for 72 h. The supernatant was collected to infect the indicated cells.

For secretion determination, cells were replaced with DMEM for 1 h or induced with 50 ng/ml LPS overnight in RPMI-1640 plus 10% FBS followed by 2 mM ATP treatment for 30 min in physiological saline solution (147 mM NaCl, 10 mM HEPES pH 7.4, 13 mM glucose, 2 mM $CaCl_2$, 1 mM $MgCl_2$, 2 mM KCl). The medium was concentrated by an Amicon filter (Millipore, UFC5010) and cell lysate was collected. Immunoblot was performed to determine the amounts of cargoes in the medium and cell. LDH assay (Thermo, 88953) was performed according to the manufacturer's protocol.

Immunofluorescence and fluorescence complementation

For immunofluorescence of cultured cells, the cells were fixed with 4% paraformaldehyde (PFA) for 15 min at room temperature, permeabilized with 0.1% TritonX-100 diluted in PBS at room temperature for 5 min, blocked with 10% FBS diluted with PBS for 1 h and primary antibody incubation for 1 h. After performing multiple washes, the samples were incubated for 40 min at room temperature with the secondary antibodies[74]. For lung tissue immunofluorescence staining, samples were fixed in 4% PFA, dehydrated in a 30% sucrose solution for 24 h, and embedded using the Tissue-Tek OCT compound. Frozen blocks were cut into 10-μm-thick sections. Fluorescence images were acquired using the Olympus FV3000 confocal microscope. Quantification was performed using ImageJ.

For fluorescence complementation, the cells expressing GFP (1-10)-TMED10-V5 and IL1β-FLAG-GFP11 were transfected with E plasmids of indicated coronaviruses. The GFP signal in the cells was collected by CytoFlex LX (Beckman) and analyzed by CytExpert software[17].

Co-immunoprecipitation and in vitro peptide/GST pull-down assay

Co-immunoprecipitation assay was performed according methods reported previously[75]. The cells were lysed on ice for 30 min in IP buffer (50 mM Tris/HCl pH 7.4, 150 mM NaCl, 1 mM EDTA, 0.5% NP40, 10% glycerol) with protease inhibitor mixture, and the lysates were cleared by centrifugation. The resulting supernatants were incubated with indicated agaroses and rotated at 4 °C for 3 h. Then the agaroses were washed five times with IP buffer followed by immunoblot.

For peptide pull-down assay, synthetic peptides were conjugated to agarose beads using the AminoLink Plus Coupling Resin (Thermo, 20501) according to the manufacturer's protocol. 2 mg purified MBP-Myc-E protein of SARS2 was incubated with 20 μL peptides-coupled beads in IP buffer and rotated at 4 °C for 3 h. Then the agarose was washed three times with IP buffer followed by immunoblot.

For GST pull-down assay, the proteins were purified and GST or GST-TMED10 was incubated with Glutathione agarose (GE, 17-0756-05) (which was blocked by 10% FBS) in IP buffer used for Co-IP, and rotated at 4 °C for 1 h. Then the beads loaded with GST or GST-TMED10 were collected and incubated with MBP-Myc-E protein of SARS2 at 4 °C for 2 h. The beads were washed 3 times followed by immunoblot.

Crosslink assay

DSS crosslink assays were performed according to the instructions of the reagents. The cells were suspended in PBS with the 0.25 mM DSS at room temperature for 30 min. The reaction was quenched with 20 mM Tris followed by sample preparation for immunoblot.

Protein purification

For protein purification, pGEX4T1-GST-TMED10, pGEX4T1-GST-Myc-E, pet28a-MBP-Myc-E, pet28a-mIL1β-flag and pGEX4T1-GST-LgBit plasmids were transformed into E.coli Rosetta (DE3), cultured at 37 °C until OD600 reach 0.5-0.8, IPTG (100 μM) induced protein expression in 22 °C for 5 h. After expression, the bacteria were collected and lysed with 0.5 mg/ml lysozyme (MP Biomedicine, 100831) in lysis buffer (2×PBS, 10 mM imidazole for His protein purification or 50 mM Tris/HCl

pH 8.0, 5 mM EDTA,150 mM NaCl, 10% glycerol for GST protein purification) plus 0.3 mM DTT and PMSF(100 μM) on ice for 30 min. Added 0.5% TritonX-100 to lysate, sonicated and centrifuged at 20,000 × g for 40 min. Incubated supernatants with Glutathione Agarose or Ni-NTA Agarose (GE, 17-5318-02) and rotated at 4 °C for 2 h. Washed the agarose with wash buffer contain 0.1% Tween20 and then wash buffer (2×PBS + 25 mM imidazole for His protein or PBS for GST protein). For purification of TMED10 and E, 0.5% Triton X-100 was included in all procedures. The proteins were eluted by elution buffer (2×PBS, 250 mM imidazole for His proteins or 50 mM Tris, pH 8.0, 250 mM KCl, 25 mM glutathione for GST proteins) and concentrated by Amicon Ultra Filters (Millipore, UFC9010). FPLC was performed for buffer exchange and increase of purity. The proteins were frozen by liquid nitrogen and stored in PBS (0.05% Triton X-100 for TMED10 and E) at -80 °C.

In vitro translocation assay

Total lipids extracted from HEK293T cells. Cell suspension and chloroform/methanol solution (methanol: chloroform = 1: 2) were mixed with a ratio 1: 4 by volume, vortexed for 30 s and shaken for 1 h at 180 rpm at 37 °C. After centrifugation at 2000 × *g* for 10 min at room temperature, chloroform phase was collected and was evaporated by a stream of nitrogen gas over the lipid solution and further dried in 37 °C incubator for 1 h. Dried lipid was suspended in HEPES-KAc buffer (20 mM HEPES, pH 7.2, 150 mM KCl). The phosphatidylcholine (PC) content of lipid solution was measured (Phospholipids C, Wako) and used as a standard to normalize lipid concentration. The lipid was aliquoted and stored in -80 °C.

For reconstitution of proteoliposomes, total lipids were frozen and thawed 10 times in liquid nitrogen and 42 °C water bath. Add 0.05% TritonX-100 into lipid solution and rotated in 4 °C for 30 min. TMED10 and E proteins were added into the lipid solution (10 μg GST-TMED10 protein, 10 μg Myc-E protein and 1.25 mg lipid in each tube) and incubated for another 1 h with rotation. Each 400 μL solution was incubated with 6–8 mg Biobeads SM2 (Bio-Rad) equilibrated with the HEPES-KAc buffer at 4 °C. Beads were replaced each hour and repeated for 5 times (10 mg beads in the third time and incubated overnight). After a 1500 × *g* centrifugation to remove the Biobeads, the liposome solution was repeatedly frozen in liquid nitrogen and thawed in 42 °C water bath for 5 times. In order to remove the free proteins, a membrane flotation procedure was performed. For each 300 μL solution, 300 μL 50% OptiPrep (diluted in HEPES-KAc buffer) was added. The mixture was overlaid with 480 mL 20% OptiPrep and 90 μl HEPES-KAc buffer, centrifuged at 45,000 rpm (TLS55) for 2 h at 4 °C and the 150 μL top fraction (which contains the proteoliposomes) was collected and diluted with 150 mM HEPES-KAc buffer.

For the in vitro translocation, IL1β protein was added to proteoliposomes (150 μL reaction system contain 6 μg IL1β), incubated for 1 h at 30 °C. After then, an equal volume of 50% OptiPrep (diluted in HEPES-KAc buffer) was added and mixed gently followed by overlaying with 240 μL 20% OptiPrep, 45 μL HEPES-KAc buffer, and centrifuged at 45,000 rpm (TLS55) for 2 h at 4 °C. The proteoliposomes (90 μL fraction from the top) were aliquoted into 3 fractions. The first fraction was a control, the second and third fractions were digested by protease K (15 μg/ml) without or with 0.5% Triton X-100 for 20 min on ice. The reactions were stopped by 1 mM PMSF and incubated for 10 min on ice. Then SDS loading buffer was added and the samples were heated at 100 °C for 10 min followed by immunoblot analysis.

Cell-free translocation assay

The cytosol of wild-type HEK293T cells was prepared followed the research methods reported in the previous literature[76]. The cells were harvested and washed with PBS followed by passing through a 22 G needle in B88 lysis buffer (20 mM HEPES-KOH, pH 7.2, 250 mM sorbitol, 150 mM potassium acetate, 5 mM magnesium acetate, protease and phosphotase inhibitors, 0.3 mM DTT). The cell homogenates were centrifuged at 100,000 × *g* for 30 min, after which the supernatant fractions were collected and stored in -80 °C. For cytosol containing GFP or GFP-ECT, HEK293T cells were transfected with the indicated plasmids. For membrane separation, the cells transfected with plasmids expressing TMED10 or different E proteins were harvested and lysed in HB1 lysis buffer (20 mM HEPES-KOH, pH 7.2, 400 mM sucrose, 1 mM EDTA, protease and phosphotase inhibitors, 0.3 mM DTT) by using a 22 G needle. The lysate was centrifuged at 3000 × *g* for 10 min and the supernatant was ultracentrifuged at 100,000 × *g* for 30 min to collect the membrane pellet. The pellet was washed with B88 and resuspended in B88 lysis buffer containing the cytosol of wild-type HEK293T cells (3 mg/ml final concentration). The phosphatidylcholine (PC) concentration was measured with a microplate spectrophotometer and adjusted to the equal concentration.

For the cell-free mIL1β translocation, recombinant proteins (120 μL reaction system contain 10 μg T7-mIL1β-flag protein), ATP regeneration system (40 mM creatine phosphate, 0.2 mg/ml creatine phosphokinase, and 1 mM ATP) and GTP (0.15 mM) were added to the purified membrane solution containing 3 mg/ml cytosol, then incubated for 1.5 h in 30 °C. After then, 100 μL reaction system was combined with 200 μL 60% OptiPrep to adjust the final concentration of OptiPrep to 40%, followed by overlaying with 600 μL 30% OptiPrep (diluted in B88 buffer), 100 μL B88 buffer, and centrifuged at 45,000 rpm (TLS55) for 2 h at 4 °C. The membrane fraction floating on the top (150 μL) was collected and aliquoted into three fractions. The first fraction was a control, the second and third fractions were digested by protease K (20 μg/ml) without or with 1% Triton X-100 for 20 min on ice, with a total volume of 40 μL per reaction. The reactions were stopped by adding PMSF and incubated for 10 min on ice. Then SDS loading buffer was added and the samples were heated at 100 °C for 10 min followed by immunoblot analysis.

AAV infection and LPS challenge

The lung-tropic AAV serotype 6 vector expressing GFP, E-SARS2, E-229E and GFP-3×ECT under the control of a CMV promoter were generated by BraninVTA Co. Ltd, China. AAVs were delivered to lung using intratracheal injection technique[38]. In brief, mice were anesthetized with avertin and a 22-gauge catheter placed into the trachea, then a total of 1×10^{11} vector genomes (vg) AAVs were administered. Four weeks later, mice received an LPS challenge (15 mg/kg) and, 15 hours following the challenge, were euthanized to collect blood serum, lung, spleen, liver, and kidney for analysis using ELISA, immunofluorescence, RT-qPCR and H&E staining.

RNA extraction and RT-qPCR

Total RNA was extracted using Trizol (Beyotime, R0016). Reverse transcription to produce cDNA was carried out by use a cDNA Reverse Transcription kit (Abclonal, RK20429), which contained 1 μg RNA in 20 μL volume. RT-qPCR was carried out by the 2×SYBR Green Master Mix (Abclonal, RK21203). Primers sequences of IL6 and GAPDH are as follows: IL6-F: TGTATGAACAACGATGATGCACTT, IL6-R: ACTCTGGC TTTGTCTTTCTTGTTATCT; GAPDH-F: GTTCCTACCCCCAATGTGTCC, GAPDH-R: TAGCCCAAGATGCCCTTCAGT.

H&E stain and inflammation evaluation

Left lobe of mice lung were fixed in 4% paraformaldehyde, paraffin embedded, and sectioned (7 μm). Tissue sections were stained with hematoxylin and eosin. The severity of lung inflammation was quantified by the percentage of inflammatory area: the area of the regions which immune cell filling to the lung alveolus and increased thickness dividing total area of lung (excluding the air space)[77].

MHV infection

Mouse hepatitis virus A59 strain (MHV-A59) was propagated and tilter was determined according to the protocol[78]. In brief, the virus was

propagated in 17Cl-1 cells, subjected to three freeze-thaw cycles between -80 °C and room temperature, centrifuged at 5000 × *g* for 20 min at 4 °C to remove cell debris, and the supernatant was then concentrated using an Amicon filter. The tilter of the virus was determined by endpoint dilution assay[78].

In the cell infection assay, 293T-mCC1a cells were firstly transfected with mIL1β plasmids and cultured for 24 h, then infected with MHV-A59 for 2 h in a serum-free medium, and subsequently cultured in a complete medium containing 10% FBS and 1% Pan-Strep for 36 h. The culture medium was then switched to DMEM for 1 h before collecting the medium to assess mIL1β secretion as described above. To evaluate the impact of drugs, BMDMs were infected with MHV-A59 (MOI 0.1), cultured for 36 h, treated with either DMSO or specific drugs for 4 h in serum-free medium, and the medium was subsequently collected to measure endogenous mIL1β secretion. To examine the impact of ECT, BMDMs underwent lentiviral infection to express either GFP or GFP-ECT and were cultured for 48 h. These cells were then infected with MHV-A59 (MOI 0.1), followed by assessment of endogenous IL1β secretion.

For mice infection assay, 8–12 weeks old IFNAR-KO mice (from Dr. Fuping You) were intranasally inoculated with MHV-A59 (2×10^4 PFU) using isoflurane as the anesthetic. The weight and health status of the mice were observed and recorded daily. Mice were euthanized at 4 dpi to collect serum and different tissues for further testing. To assess drug efficacy, mice were first infected with MHV and then received intraperitoneal injections of DMSO, UPA (1 mg/kg), or Progesterone (1 mg/kg) for three consecutive days, with euthanasia occurring on the fourth day post-infection. Regarding AAV infection, mice underwent initial infection with either AAV-GFP or AAV-GFP-ECT, followed by MHV infection four weeks later.

Compound screening

Rapid secretion analysis assay using complementary NanoLuc leuciferace was employed to screen inhibitors for E-SARS2-induced mIL1β secretion[53]. 100 nL of compounds and DMSO or H_2O controls were added to 96-well plate by Echo 650 Liquid Handler (Beckman). HEK293T cell expression mIL1β-HiBiT and Myc-E-SARS2 were seeded to a 96-well plate, and cultured at 37 °C for 8 h. The medium was collected and each 30 μL medium incubated with Furimazine (10 nM final concentration) and 5 ng LgBit protein in a 60 μL reaction system at room temperature for 10 min. Luminescence was detected using EnSpire Multimode Plate Reader (PerkinElmer). Compounds with fluorescence intensity decreased by more than 0.75-fold relative to control in two independent experiments were selected as candidates.

Statistics and reproducibility

Statistics analyzes were performed using GraphPad Prism 8.0. Micrographs in Fig. 2a, b, and Supplementary Fig S4a are representatives of three independent experiments and were acquired randomly. All blot data are representative of at least three independent experiments.

Reporting summary

Further information on research design is available in the Nature Portfolio Reporting Summary linked to this article.

Data availability

All data supporting the findings of this study are presented in the paper, Supplementary Information or Source Data file. All data and strains are available upon request. Source data are provided with this paper.

References

1. Tay, M. Z., Poh, C. M., Rénia, L., MacAry, P. A. & Ng, L. F. The trinity of COVID-19: immunity, inflammation and intervention. *Nat. Rev. Immunol.* **20**, 363–374 (2020).
2. De Wit, E., Van Doremalen, N., Falzarano, D. & Munster, V. J. SARS and MERS: recent insights into emerging coronaviruses. *Nat. Rev. Microbiol.* **14**, 523–534 (2016).
3. Zhang, Y.-y, Li, B.-r & Ning, B.-t The comparative immunological characteristics of SARS-CoV, MERS-CoV, and SARS-CoV-2 coronavirus infections. *Front. Immunol.* **11**, 2033 (2020).
4. Del Valle, D. M. et al. An inflammatory cytokine signature predicts COVID-19 severity and survival. *Nat. Med.* **26**, 1636–1643 (2020).
5. Xia, B. et al. SARS-CoV-2 envelope protein causes acute respiratory distress syndrome (ARDS)-like pathological damages and constitutes an antiviral target. *Cell Res.* **31**, 847–860 (2021).
6. Yang, L. et al. COVID-19: immunopathogenesis and Immunotherapeutics. *Signal Transduct. Target. Ther.* **5**, 128 (2020).
7. Hu, B., Huang, S. & Yin, L. The cytokine storm and COVID-19. *J. Med. Virol.* **93**, 250–256 (2021).
8. Tan, M. et al. Immunopathological characteristics of coronavirus disease 2019 cases in Guangzhou, China. *Immunology* **160**, 261–268 (2020).
9. Qin, C. et al. Dysregulation of immune response in patients with coronavirus 2019 (COVID-19) in Wuhan, China. *Clin. Infect. Dis.* **71**, 762–768 (2020).
10. Mantovani, A., Dinarello, C. A., Molgora, M. & Garlanda, C. Interleukin-1 and related cytokines in the regulation of inflammation and immunity. *Immunity* **50**, 778-795, https://doi.org/10.1016/j.immuni.2019.03.012 (2019).
11. Kaneko, N., Kurata, M., Yamamoto, T., Morikawa, S. & Masumoto, J. The role of interleukin-1 in general pathology. *Inflamm. regeneration* **39**, 1–16 (2019).
12. Griesenauer, B. & Paczesny, S. The ST2/IL-33 axis in immune cells during inflammatory diseases. *Front. Immunol.* **8**, 475 (2017).
13. Markovic, S. S. et al. IL 33 correlates with COVID-19 severity, radiographic and clinical finding. *Front. Med.* **8**, 749569 (2021).
14. Conti, P. et al. Coronavirus-19 (SARS-CoV-2) induces acute severe lung inflammation via IL-1 causing cytokine storm in COVID-19: a promising inhibitory strategy. *J. Biol. Regul. Homeost. Agents* **34**, 1971–1975 (2020).
15. Makaremi, S. et al. The role of IL-1 family of cytokines and receptors in pathogenesis of COVID-19. *Inflamm. Res.* **71**, 923–947 (2022).
16. Monteleone, M., Stow, J. L. & Schroder, K. Mechanisms of unconventional secretion of IL-1 family cytokines. *Cytokine* **74**, 213–218 (2015).
17. Zhang, M. et al. A translocation pathway for vesicle-mediated unconventional protein secretion. *Cell* **181**, 637–652.e615 (2020).
18. Zhang, M. & Schekman, R. Unconventional secretion, unconventional solutions. *Science* **340**, 559–561 (2013).
19. Evavold, C. L. et al. The pore-forming protein gasdermin D regulates interleukin-1 secretion from living macrophages. *Immunity* **48**, 35–44.e36 (2018).
20. Kayagaki, N. et al. Caspase-11 cleaves gasdermin D for non-canonical inflammasome signalling. *Nature* **526**, 666–671 (2015).
21. Shi, J. et al. Cleavage of GSDMD by inflammatory caspases determines pyroptotic cell death. *Nature* **526**, 660–665 (2015).
22. Chen, W. et al. Allergen protease-activated stress granule assembly and gasdermin D fragmentation control interleukin-33 secretion. *Nat. Immunol.* **23**, 1021–1030 (2022).
23. Yang, L. et al. Intraepithelial mast cells drive gasdermin C-mediated type 2 immunity. *Immunity* **57**, 1056–1070.e1055 (2024).
24. Dupont, N. et al. Autophagy-based unconventional secretory pathway for extracellular delivery of IL-1β. *EMBO J.* **30**, 4701–4711 (2011).
25. Martín-Sánchez, F. et al. Inflammasome-dependent IL-1β release depends upon membrane permeabilisation. *Cell Death Differ.* **23**, 1219–1231 (2016).
26. Monteleone, M. et al. Interleukin-1β maturation triggers its relocation to the plasma membrane for gasdermin-D-dependent and-independent secretion. *Cell Rep.* **24**, 1425–1433 (2018).

27. Su, S. et al. Epidemiology, genetic recombination, and pathogenesis of coronaviruses. *Trends Microbiol.* **24**, 490–502 (2016).
28. He, F., Deng, Y. & Li, W. Coronavirus disease 2019: What we know? *J. Med. Virol.* **92**, 719–725 (2020).
29. Fung, T. S. & Liu, D. X. Human coronavirus: host-pathogen interaction. *Annu. Rev. Microbiol.* **73**, 529–557 (2019).
30. Stertz, S. et al. The intracellular sites of early replication and budding of SARS-coronavirus. *Virology* **361**, 304–315 (2007).
31. Schoeman, D. & Fielding, B. C. Coronavirus envelope protein: current knowledge. *Virol. J.* **16**, 1–22 (2019).
32. Venkatagopalan, P., Daskalova, S. M., Lopez, L. A., Dolezal, K. A. & Hogue, B. G. Coronavirus envelope (E) protein remains at the site of assembly. *Virology* **478**, 75–85 (2015).
33. Wang, Y. et al. TMED10-mediated unconventional secretion of IL-33 regulates intestinal epithelium differentiation and homeostasis. *Cell Res.* 1-4 https://doi.org/10.1038/s41422-023-00891-3 (2024).
34. Zhang, M., Kenny, S. J., Ge, L., Xu, K. & Schekman, R. Translocation of interleukin-1β into a vesicle intermediate in autophagy-mediated secretion. *elife* **4**, e11205 (2015).
35. Vora, S. M., Lieberman, J. & Wu, H. Inflammasome activation at the crux of severe COVID-19. *Nat. Rev. Immunol.* **21**, 694–703 (2021).
36. Sun, X. et al. SARS-CoV-2 non-structural protein 6 triggers NLRP3-dependent pyroptosis by targeting ATP6AP1. *Cell Death Differ.* **29**, 1240–1254 (2022).
37. Ferreira, A. C. et al. SARS-CoV-2 engages inflammasome and pyroptosis in human primary monocytes. *Cell death Discov.* **7**, 43 (2021).
38. Santry, L. A. et al. AAV vector distribution in the mouse respiratory tract following four different methods of administration. *BMC Biotechnol.* **17**, 1–11 (2017).
39. Mandala, V. S. et al. Structure and drug binding of the SARS-CoV-2 envelope protein transmembrane domain in lipid bilayers. *Nat. Struct. Mol. Biol.* **27**, 1202–1208 (2020).
40. Surya, W., Li, Y., Verdià-Bàguena, C., Aguilella, V. M. & Torres, J. MERS coronavirus envelope protein has a single transmembrane domain that forms pentameric ion channels. *Virus Res.* **201**, 61–66 (2015).
41. Verdiá-Báguena, C. et al. Coronavirus E protein forms ion channels with functionally and structurally-involved membrane lipids. *Virology* **432**, 485–494 (2012).
42. Wang, Y. et al. Impact of SARS-CoV-2 envelope protein mutations on the pathogenicity of Omicron XBB. *Cell Discov.* **9**, 80 (2023).
43. Wang, W.-A., Carreras-Sureda, A. & Demaurex, N. SARS-CoV-2 infection alkalinizes the ERGIC and lysosomes through the viroporin activity of the viral envelope protein. *J. Cell Sci.* **136**, jcs260685 (2023).
44. Nieto-Torres, J. L. et al. Severe acute respiratory syndrome coronavirus E protein transports calcium ions and activates the NLRP3 inflammasome. *Virology* **485**, 330–339 (2015).
45. Yalcinkaya, M. et al. Modulation of the NLRP3 inflammasome by Sars-CoV-2 Envelope protein. *Sci. Rep.* **11**, 24432 (2021).
46. Nieto-Torres, J. L. et al. Severe acute respiratory syndrome coronavirus envelope protein ion channel activity promotes virus fitness and pathogenesis. *PLoS Pathog.* **10**, e1004077 (2014).
47. Pervushin, K. et al. Structure and inhibition of the SARS coronavirus envelope protein ion channel. *PLoS Pathog.* **5**, e1000511 (2009).
48. Regla-Nava, J. A. et al. Severe acute respiratory syndrome coronaviruses with mutations in the E protein are attenuated and promising vaccine candidates. *J. Virol.* **89**, 3870–3887 (2015).
49. Hossain, A., Akter, S., Rashid, A. A., Khair, S. & Alam, A. R. U. Unique mutations in SARS-CoV-2 Omicron subvariants' non-spike proteins: Potential impacts on viral pathogenesis and host immune evasion. *Microb. pathogenesis* **170**, 105699 (2022).
50. Shuai, H. et al. Attenuated replication and pathogenicity of SARS-CoV-2 B.1.1.529 Omicron. *Nature* **603**, 693–699 (2022).
51. Bálint, G., Vörös-Horváth, B. & Széchenyi, A. Omicron: increased transmissibility and decreased pathogenicity. *Signal Transduct. Target. Ther.* **7**, 151 (2022).
52. Nieto-Torres, J. L. et al. Subcellular location and topology of severe acute respiratory syndrome coronavirus envelope protein. *Virology* **415**, 69–82 (2011).
53. Schwinn, M. K. et al. CRISPR-mediated tagging of endogenous proteins with a luminescent peptide. *ACS Chem. Biol.* **13**, 467–474 (2018).
54. Ghosh, S. et al. β-Coronaviruses use lysosomes for egress instead of the biosynthetic secretory pathway. *Cell* **183**, 1520–1535.e1514 (2020).
55. Guo, Q. et al. Induction of alarmin S100A8/A9 mediates activation of aberrant neutrophils in the pathogenesis of COVID-19. *Cell host microbe* **29**, 222–235.e224 (2021).
56. Sharma, L. et al. Distinct roles of type I and type III interferons during a native murine β coronavirus lung infection. *J. Virol.* **96**, e01241–01221 (2022).
57. Yuan, L. et al. Female sex hormone, progesterone, ameliorates the severity of SARS-CoV-2-caused pneumonia in the Syrian hamster model. *Signal Transduct. Target. Ther.* **7**, 47 (2022).
58. Su, S. et al. Modulation of innate immune response to viruses including SARS-CoV-2 by progesterone. *Signal Transduct. Target. Ther.* **7**, 137 (2022).
59. Zhou, S. et al. SARS-CoV-2 E protein: Pathogenesis and potential therapeutic development. *Biomed. Pharmacother.*, 114242 (2023).
60. Schoeman, D. & Fielding, B. C. Is there a link between the pathogenic human coronavirus envelope protein and immunopathology? A review of the literature. *Front. Microbiol.* **11**, 2086 (2020).
61. Zheng, M. et al. TLR2 senses the SARS-CoV-2 envelope protein to produce inflammatory cytokines. *Nat. Immunol.* **22**, 829–838 (2021).
62. De Maio, F. et al. Improved binding of SARS-CoV-2 Envelope protein to tight junction-associated PALS1 could play a key role in COVID-19 pathogenesis. *Microbes Infect.* **22**, 592–597 (2020).
63. Chai, J. et al. Structural basis for SARS-CoV-2 envelope protein recognition of human cell junction protein PALS1. *Nat. Commun.* **12**, 3433 (2021).
64. Lin, X. et al. Unconventional secretion of unglycosylated ORF8 is critical for the cytokine storm during SARS-CoV-2 infection. *PLoS Pathog.* **19**, e1011128 (2023).
65. Matsuoka, K. et al. SARS-CoV-2 accessory protein ORF8 is secreted extracellularly as a glycoprotein homodimer. *J. Biol. Chem.* **298**, 101724 (2022).
66. Lin, X. et al. ORF8 contributes to cytokine storm during SARS-CoV-2 infection by activating IL-17 pathway. *Iscience* **24**, 102293 (2021).
67. Miao, G. et al. ORF3a of the COVID-19 virus SARS-CoV-2 blocks HOPS complex-mediated assembly of the SNARE complex required for autolysosome formation. *Developmental cell* **56**, 427–442.e425 (2021).
68. Ji, M. et al. VMP1 and TMEM41B are essential for DMV formation during β-coronavirus infection. *J. Cell Biol.* **221**, e202112081 (2022).
69. Trimarco, J. D. et al. TMEM41B is a host factor required for the replication of diverse coronaviruses including SARS-CoV-2. *PLoS Pathog.* **17**, e1009599 (2021).
70. Schneider, W. M. et al. Genome-scale identification of SARS-CoV-2 and pan-coronavirus host factor networks. *Cell* **184**, 120–132.e114 (2021).
71. Mukherjee, S. & Pahan, K. Is COVID-19 gender-sensitive? *J. Neuroimmune Pharmacol.* **16**, 38–47 (2021).
72. Zhang, J. et al. A systemic and molecular study of subcellular localization of SARS-CoV-2 proteins. *Signal Transduct. Target. Ther.* **5**, 269 (2020).
73. Hu, X. et al. Integrated regulation of Toll-like receptor responses by Notch and interferon-γ pathways. *Immunity* **29**, 691–703 (2008).

74. Li, S. et al. A new type of ERGIC–ERES membrane contact mediated by TMED9 and SEC12 is required for autophagosome biogenesis. *Cell Res.* **32**, 119–138 (2022).
75. Ma, X. et al. CCT2 is an aggrephagy receptor for clearance of solid protein aggregates. *Cell* **185**, 1325–1345.e1322 (2022).
76. Ge, L., Melville, D., Zhang, M. & Schekman, R. The ER–Golgi intermediate compartment is a key membrane source for the LC3 lipidation step of autophagosome biogenesis. *elife* **2**, e00947 (2013).
77. Lopera, D. et al. Structural and topographic dynamics of pulmonary histopathology and local cytokine profiles in Paracoccidioides brasiliensis conidia-infected mice. *PLoS Neglected Tropical Dis.* **5**, e1232 (2011).
78. Leibowitz, J., Kaufman, G. & Liu, P. Coronaviruses: propagation, quantification, storage, and construction of recombinant mouse hepatitis virus. *Curr. Protoc. Microbiol.* **21**, 15E. 11.11–15E. 11.46 (2011).

Acknowledgements

We thank Dr. Feng Shao (National Institute of Biological Sciences, China) for GSDMD-KO mice, Dr. Fuping You (Peking University, China) for IFNAR-KO mice and MHV-A59. We thank Dr. Xiaoyu Hu (Tsinghua University, China) for the assistant of experimental technique. We thank Dr. Zhaobing Gao and Dr. Bingqing Xia (Chinese Academy of Sciences, China) for suggestions on this project. We thank Dr. Ziyi Guo, Dr. Fengwu Chen, Qing Guo, Xiangyue Mu for the help of mice experiment. This work is funded by National Natural Science Foundation of China (32370728), Vanke Special Fund for Public Health and Health Discipline Development, Tsinghua University (2022Z82WKJ009), National Natural Science Foundation of China (92254302, 32225013, 32200553, 32130023), Tsinghua University Dushi Program, Tsinghua University Initiative Scientific Research Program (No.20221080048, No.20231080030).

Author contributions

M.Z. and L.G. conceived the project. L.L., L.Z., P.W., and M.Z. performed cell and biochemical experiments. L.L., L.Z., and Y.W. performed AAV infection experiments. L.L. and L.Z. performed drug screening experiments. X.Z and B.T performed the bioinformatics analysis to search the analogs of progesterone. L.L., L.Z., and X.H. performed the MHV infection experiments. L.L., L.Z., and M.Z. analyzed the data. M.Z., L.G., L.L., and L.Z. wrote the manuscript.

Competing interests

The authors declare no competing interests.

Additional information

Supplementary information The online version contains supplementary material available at https://doi.org/10.1038/s41467-024-52818-0.

Correspondence and requests for materials should be addressed to Min Zhang.

Peer review information *Nature Communications* thanks the anonymous reviewer(s) for their contribution to the peer review of this work. A peer review file is available.